Open access • Journal Article • DOI:10.1021/ACSAMI.0C06865

Zinc-Calcium-Fluoride Bioglass-Based Innovative Multifunctional Dental Adhesive with Thick Adhesive Resin Film Thickness. — Source link

Chenmin Yao, Chenmin Yao, Mohammed H Ahmed, Mohammed H Ahmed ...+9 more authors

Institutions: Wuhan University, Katholieke Universiteit Leuven, Tanta University, Academic Center for Dentistry Amsterdam ...+1 more institutions

Published on: 12 Jun 2020 - ACS Applied Materials & Interfaces (American Chemical Society)

Topics: Adhesive, Bond strength, Dentin and Chemical binding

Zinc-calcium-fluoride bioglass-based innovative multi-functional dental adhesive with thick adhesive-resin film thickness

Chenmin Yao,[†,‡] Mohammed H. Ahmed,[†,§] Xin Li,[†] Ivana Nedeljkovic,[†,//] Jennifer Vandooren,[#] Ben Mercelis,[†] Fei Zhang,[†,&] Kirsten L. Van Landuyt,[†] Cui Huang,[‡] Bart Van Meerbeek[†,*]

[†]KU Leuven (University of Leuven), Department of Oral Health Sciences, BIOMAT & UZ Leuven (University Hospitals Leuven), Dentistry, 3000 Leuven, Belgium;

[‡]Wuhan University, the State Key Laboratory Breeding Base of Basic Science of Stomatology (Hubei-MOST) & Key Laboratory of Oral Biomedicine Ministry of Education (KLOBM), School & Hospital of Stomatology, 430079 Wuhan, China;

[§]Tanta University, Faculty of Dentistry, Department of Dental Biomaterials, 31511 Tanta, Egypt;

[//]University of Amsterdam and Vrije Universiteit Amsterdam, Department of Dental Material Sciences, Academic Centre for Dentistry Amsterdam (ACTA), 1081 LA Amsterdam, The Netherlands;

[#]KU Leuven (University of Leuven), Laboratory of Immunobiology, Rega Institute for Medical Research, 3000 Leuven, Belgium;

[&]KU Leuven (University of Leuven), Department of Materials Engineering, 3001 Leuven, Belgium.

*Corresponding author.

Chenmin Yao, Mohammed H. Ahmed, Xin Li, Ivana Nedeljkovic, Jennifer Vandooren, Ben Mercelis, Fei Zhang, Kirsten L. Van Landuyt, Cui Huang, Bart Van Meerbeek. Zinc-calcium-fluoride bioglass-based innovative multi-functional dental adhesive with thick adhesive-resin film thickness. ACS Applied Materials & Interfaces.

ABSTRACT: Apart from producing high bond strength to tooth enamel and dentin, a dental adhesive with bio-therapeutic potential is clinically desirable, aiming to further improve tooth-restoration longevity. In this laboratory study, an experimental two-step universal adhesive, being referred to as Exp_2UA, applicable in both etch-and-rinse (E&R) and self-etch (SE) mode and combining a primer, containing 10-methacryloyloxydecyldihydrogen phosphate (10-MDP) as functional monomer with

chemical binding potential to hydroxyapatite, with a bioglass-containing hydrophobic adhesive resin, was multifactorially investigated. In addition to primary property assessment, including measurement of bond strength, water sorption, solubility and polymerization efficiency, the resultant adhesive-dentin interface was characterized by TEM, the filler composition analyzed by EDS and the adhesive's bioactive potential estimated by measuring long-term ion release and assessing its anti-enzymatic and anti-bacterial potential. Four representative commercial adhesives served as reference/controls. Application in both E&R and SE mode resulted in durable bonding performance to dentin, as evidenced by favorable 1-year aged bond-strength data and a tight interfacial ultra-structure that, as examined by TEM, remained ultra-morphologically unaltered upon 1-year water-storage aging. TEM revealed a 20-µm thick hydrophobic adhesive layer with a homogeneous bioglass filler distribution. Adequate polymerization conversion resulted in extremely low water sorption and solubility. *In-situ* zymography revealed reduced endogenous proteolytic activity, while *Streptococcus mutans* biofilm formation was inhibited. In conclusion, the three/two-step E&R/SE Exp_2UA combines high bonding potential and bond-degradation resistance with long-term ion release rendering the adhesive anti-enzymatic and anti-bacterial potential.

KEYWORDS: bioactive; ion release; anti-enzymatic; anti-bacterial; bond durability; adhesive-dentin interface; methacryloxydecyl dihydrogen phosphate

1. INTRODUCTION

The use of dental adhesives to bond tooth-colored resin-based composites (RBC) to tooth tissue, so enabling to minimally invasively restore teeth, has revolutionized today's dental practice, hereby closely meeting each patient's major demand for aesthetic and nearly invisible tooth restorations. The RBC restoration's longevity depends highly on the clinical performance of dental adhesives, bonding the restorative composite to tooth enamel and dentin. In a challenging humid mouth, tooth restorations are cyclically subjected/exposed to mechanical stress during chewing, temperature changes and acid attacks, as well as bacterial cariogenic effects during continuous biofilm activity.

The fundamental principle of adhesion is based on a biomaterial-tooth exchange process, involving substitution of inorganic tooth material by synthetic resin monomers that upon *in-situ* polymerization micro-mechanically interlock within beforehand created surface micro-retention.[1] This exchange

process can be conducted following an etch-and-rinse (E&R) or self-etch (SE) bonding approach.[2-3] Diffusion-based micro-mechanical interlocking within a fully demineralized collagen-rich and hydroxyapatite-free 3- to 5-µm hybrid layer constitutes the primary bonding mechanism of adhesives employed in an E&R bonding mode.[4] Adhesives employed in a mild SE bonding mode make additionally use of primary ionic interaction of dedicated functional monomers with hydroxyapatite within a partially demineralized submicron hybrid layer. Additional chemical binding is thought to contribute in particular to bond durability.[4] Both the E&R and SE bonding modes have potential, especially when applied in a multi-step application procedure, but they also have limitations.[2-4]

So-called universal adhesives (UAs) represent the newest generation of dental adhesives. They are rapidly becoming popular in today's clinical practice because of their ease of use and two bonding mode options.[5] Based on the primary bonding mechanisms mentioned above, UAs most effectively bond to tooth tissue by combining selective phosphoric-acid etching of enamel with a successive SE bonding routine applied both on the beforehand etched enamel and non-etched dentin.[4] Nevertheless, UAs should be considered as trade-off adhesives by combining the primer and adhesive resin into a single solution. Major drawbacks of UAs are their relatively high hydrophilic nature and thin film thickness, reducing their interfacial stress-absorbing potential and potentially compromising their long-term clinical bonding performance, which due to lack of long-term clinical data is not yet known.[4]

Simplified adhesive procedures should however not compromise clinical bonding performance.[6-7] Previous generation one-step adhesives as well as the newest generation of UAs have repeatedly *in vitro* been proven to benefit from an extra hydrophobic adhesive layer, basically transforming their two-step E&R bonding mode into a three-step E&R bonding mode or their one-step SE bonding mode into a two-step SE bonding mode.[8-10] In fact, these extended application procedures resemble those of the respective gold-standard three-step E&R and two-step SE adhesives.[4] Besides thicker film thickness to better stabilize the adhesive interface with enhanced interfacial stress-absorbing potential, the improved bonding performance of the multi-step application procedure should be attributed to the higher interfacial hydrophobicity achieved and improved sealing of the adhesive interface, protecting it better against water uptake through osmosis from the underlying dentin as well as the outer oral environment. Water sorption resulting in hydrolysis should most likely be regarded as the main bond-degradation mechanism of adhesive-dentin interfaces.[11]

In addition, scientific literature has richly documented the sensitivity of adhesive-dentin interfaces to enzymatic bio-degradation processes.[12-13] Acidic dental bonding procedures have been demonstrated to not only expose but also activate dentinal enzymes,[14-15] with a higher exposure/activity recorded following an E&R than (mild) SE bonding mode.[4,14-15] Previous research identified the presence of several MMPs within dentin, among which the gelatinases MMP-2 and MMP-9, and the collagenase MMP-8 have been described to be involved most in bond degradation at human dentin.[14,16-17] In response to these findings, several exogenous inhibitors of MMPs have been investigated on their MMP-inhibiting contribution to bond stability, among which chlorhexidine was studied most frequently.[18] Subsequent research has also promoted the use of collagen cross-linkers that besides anti-enzymatic effects make exposed collagen more resistant against degradation.[19] Although zinc at physiological concentrations is a necessary element for collagen hydrolysis by MMPs,[20] zinc was also reported to act as a potential MMP inhibitor at high concentrations.[21] Especially MMP-2 and MMP-9 are inhibited by zinc and other metals.[22-23] Loading an adhesive with zinc that can gradually be released to the immediate dentin environment may help to retard biodegradation of adhesive interfaces.

Secondary caries is the principal cause of dental restoration failure and a major clinical challenge for dental RBC's.[24] Prevalence of secondary caries was found to be higher with composite than amalgam restorations, regardless of the patient's caries-risk status.[24] In this light, there is currently a research trend towards developing dental adhesives (and restorative materials) with anti-bacterial potential. The commercial adhesive scientifically documented most with laboratory research revealing anti-bacterial effects is Clearfil SE Protect (Kuraray Noritake, Tokyo, Japan). This adhesive contains the anti-bacterial monomer 12-methacryloyloxy dodecypyridinium bromide (MDPB), which later appeared also to possess anti-MMP activity.[25] Clinical evidence if such additional therapeutic effects prolong the lifetime of adhesive tooth restorations is unfortunately still insufficiently convincing.[26] Other studies ascribed anti-bacterial effects of restorative (and luting) materials to a gradual and continuous release of ions like zinc[27] and fluoride[28]. This approach has stimulated dental materials scientists to load resin-based materials with active bioglass filler particles; such materials could slowly and continuously release anti-bacterial ions to the restoration's immediate environment with potential to inhibit biofilm development and growth. Generally, the main function of filler particles is to enhance the material's mechanical properties. Additional bio-functional, anti-bacterial and anti-MMP performance of ion-

releasing filler particles added to dental adhesives (and restorative RBCs) on dentin bonding has insufficiently been addressed scientifically. Whereas the design and development of bioactive dental adhesives that release ions may not be difficult, combining 'bioactivity' with 'mechanical stability' presents a considerable challenge.[4]

In this study, we investigated a new experimentally designed and developed multi-functional UA that was intended to combine better resistance against hydrolytic bond-degradation processes with additional bioactive potential in light of the clinically highly desired anti-bacterial and anti-MMP properties. The null hypotheses tested were that (1) water sorption and solubility, and (2) polymerization efficiency of the new multi-functional adhesive was at least statistically equivalent to those of the reference adhesives, (3) the 'immediate' and 'aged' bonding efficacy to dentin of the new multi-functional adhesive did not significantly underscore those obtained by the reference adhesives, and that the new multi-functional adhesive possessed anti-MMP (4) and anti-bacterial (5) bioactive potential.

2. EXPERIMENTAL SECTION

2.1. Experimental two-step UA and commercial reference adhesives. The experimental two-step UA, further being referred to as 'Exp_2UA', combines an experimental primer based on technology of the commercial UA G-Premio Bond ('G-PrBp', GC), used as primer without being separately light-cured, with an experimental particle-filled adhesive resin synthesized by GC under the code name 'BZF-21' (Tokyo, Japan). The basic composition is detailed in Table S1. Noteworthy is that both the primer and adhesive resin do not contain the highly hydrophilic monomer 2-hydroxyethyl methacrylate (HEMA), while the adhesive resin contains zinc-calcium-fluoride bioglass and fumed silica filler.

Representing the adhesive generation of UAs, the commercial products G-Premio Bond ('G-PrB', GC), Prime&Bond Active ('P&Ba'; Dentsply Sirona, Konstanz, Germany) and Scotchbond Universal ('SBU'; 3M Oral Care, Seefeld, Germany), and the gold-standard two-step self-etch adhesive Clearfil SE Bond 2 ('CSE2'; Kuraray Noritake) served as reference (control) adhesives.

2.2. Scanning transmission electron microscopy with energy-dispersive X-ray spectroscopy (STEM/EDS) of the experimental adhesive resin BZF-21. To reveal the adhesive's ultra-structure, TEM

silicon molds (AGG3531-1, Agar Scientific, Essex, UK), commonly used to embed specimens in epoxy resin prior to TEM ultra-microtomy, were filled with the experimental particle-filled adhesive resin BZF-21 and light-cured for 60 sec (s) at both sides using a polywave light-emitting diode (LED) curing light (Bluephase 20i, Ivoclar Vivadent, Schaan, Liechtenstein; used in 'high mode': 1200 mW/cm^2, as confirmed using Marc Resin Calibrator (BlueLight Analytics, Halifax, Canada).[29] Upon storage for 6 hours (h) in a 37°C incubator, ultra-thin (10-20 nm) sections were cut using an ultramicrotome (Ultracut UCT, Leica, Vienna, Austria) and observed by STEM (JEM-ARM200F, Jeol, Tokyo, Japan) at 200 kV. Selected areas were chemically mapped with EDS utilizing a Silicon Drift Detector (Centurio, Jeol).

2.3. Ion release of the experimental adhesive resin BZF-21. Resin disks (n=58) with a 10-mm diameter and 2-mm thickness[30] were made by filling silicone molds (Aquasil medium body, Dentsply Sirona) with the experimental particle-filled adhesive resin BZF-21. The molds were protected with a thin glass slide to avoid polymerization inhibition by oxygen, upon which the disks were light-cured at the center for 60s from top and bottom sides using the LED-curing light (Bluephase 20i) used in 'high mode'. Additionally, the disks were light cured for 5s from the four sides, so to ensure optimum curing, totaling to a light-curing time of 140s (light dose: 168,000 mWs/cm^2). Next, the top and bottom surfaces were wet ground with P1200 silicon carbide (SiC) paper (Struers, Ballerup, Denmark) to adjust the disk thickness. Each specimen (n=24) was immersed in 3 ml Milli-Q water (Synergy, Millipore SAS, Molsheim, France). The concentrations of zinc (Zn) and calcium (Ca) released from the disks were measured using Inductivity Coupled Plasma - Optical Emission Spectroscopy (ICP-OES; Varian 720 ES, Varian, Palo Alto, CA, USA) after 1, 4, 7, 14, 21, 28 days (d), 6 months (6m) and 1 year (1y). The Zn and Ca ion-release concentration was calculated in function of time in ppm.

Because ICP-OES cannot measure fluoride (F), the remaining specimens (n=24) were each immersed in 5 ml Milli-Q water, upon which F release was measured by an ion-specific electrode (SevenCompact pH/ion S220, Mettler Toledo, Columbus, USA). The F ion-release concentrations released from the specimens were measured after 1, 4, 7, 14, 21, 28d, 6m and 1y. Sample solutions were diluted with a same solution amount of total ionic adjustment buffer (TISAB II with CDTA, Mettler Toledo, Im Langacher, Greifensee, Switzerland).

To avoid a saturation effect, ion release from another 10 resin disks (5 disks for Zn and Ca ion release and 5 disks for F ion release) was measured. The solution (sterilized Milli-Q water) was collected after

1d, and 1, 2, 3 and 4 weeks (w) with the solution changed every week. The ion-release concentrations were calculated in function of the area (in μg/mm^2/d).

2.4. Water sorption and solubility of the experimental adhesive resin BZF-21 and reference adhesives. Water sorption and solubility of the adhesives after 7d, 6m and 1y water immersion were measured using a weighing method, as used before.[31-32] Nine disks with a 15-mm diameter and 1-mm thickness of the experimental adhesive resin BZF-21, the reference UAs G-PrB, P&Ba, and SBU, and the adhesive resin ('Bond') of CSE2 were prepared using silicone molds. The size of the resin disks in this section was prepared according to the ISO 4049:2019(E) standard.[33] The silicone mold containing adhesive was left undisturbed in a dark box for 30s prior to light curing, so to enable solvent to evaporate. The resin disks were light-cured at the center for 60s and additionally at the periphery for 20s (four overlapping zones exposed to light for 5s each), this at both sides using the LED-curing light Bluephase 20i (Ivoclar Vivadent). Hence, the total light-curing time per specimen was 160s (light dose: 192,000 mWs/cm^2). Further measurement details are described in the Supporting Information. The water sorption (Wsp) and solubility (Wsl) in μg/mm^3 were calculated as follows:

$$Wsp = \frac{m2-m3}{V} \quad (1)$$

$$Wsl = \frac{m1-m3}{V} \quad (2)$$

where m1 is the initial dry mass before immersion into water (expressed in mg), m2 is the mass after immersion, and m3 is the mass that specimens have gained upon maximum water sorption, while v is the specimen volume (expressed in mm^3).

2.5. Real-time degree of (polymerization) conversion (DC) of the experimental two-step UA Exp_2UA and reference adhesives. A total of 15 non-carious human third molars (n=3 per adhesive) were collected following informed consent approved by the Commission for Medical ethics of KU Leuven (File number: S54254; counting for all following project parts using human teeth). The mid-coronal dentin surface was split into two equal parts by cutting a groove of 0.3-mm width and 2.5-mm depth using a slow-speed diamond saw (Micracut 151, Metkon, Bursa, Turkey). A standard bur-cut smear layer was produced, as detailed before[29] (the preparation steps are detailed in the Supporting Information). The tooth specimens were then sectioned parallel to the dentin surface to obtain two

dentin disk halves with a 2-mm thickness. Next, 5 µl of the experimental BZF-21 adhesive resin and the commercial CSE2 adhesive resin ('Bond') were applied on dentin disk halves, which were beforehand primed with G-PrBp and CSE2 primer, respectively. The reference UAs G-PrB, P&Ba and SBU were directly applied on dentin disk halves. Besides being used in SE mode, all adhesives were also used in E&R mode using 35% phosphoric acid (K-etchant, Kuraray Noritake).

The abundantly applied adhesive resins were covered by a thin glass slide with a thickness of 70-80 µm and light-cured for 10s using the LED-curing light Bluephase 20i (Ivoclar Vivadent). The degree of (polymerization) conversion (DC) was measured using micro-Raman spectroscopy (Senterra, Bruker, Ettlingen, Germany) by a near-infrared laser with a wavelength of 785 nm and used with an output power of 100 mW.[34] The laser was focused through a 50× microscope objective and a 50 × 1000-µm aperture in a slit mode. Micro-Raman spectra of the adhesive-covered dentin disks were continuously acquired for 20 minutes (min) after light curing. The collected spectra were obtained over the region of 50-3500 cm^{-1} with a resolution of 9-15 cm^{-1}. The integration time was set to 20s with 2 co-additions, all following a methodology described before.[34] The results were analyzed using OPUS 7.0 software (Bruker, Ettlingen, Germany). DC was calculated as follows:

$$DC = \left(1 - \frac{Rcured}{Runcured}\right) \times 100 \qquad (3)$$

where R is the ratio of peak intensity of the 1639-cm^{-1} (aliphatic C=C bond) and 1609-cm^{-1} (aromatic C=C bond) peaks in the spectra of Exp_2UA, G-PrB, SBU and CSE2, and of the 1639-cm^{-1} (aliphatic C=C bond) and 1458cm^{-1} (C-H bond) peaks in the spectra of the bisacrylamide-based adhesive P&Ba.[35] All handling conducted within the micro-Raman device were protected from ambient light by using orange-filtered light.[36] The differences between the groups' maximum DC were analyzed using two-way analysis of variance (ANOVA) for the two factors 'adhesive' and 'bonding mode'.

2.6. Micro-tensile bond strength (µTBS) to dentin of the experimental two-step UA Exp_2UA and reference adhesives. Fifty (n=10 per experimental group) non-carious human third molars were prepared for µTBS testing. The mid-coronal dentin surface was superficially split into two equal parts by cutting a shallow groove of 0.3-mm width and 0.5-mm depth. A standard bur-cut smear layer was produced as aforementioned. After positioning a thin razor blade (009 RD single edge carbon steel, American Safety Razor, Virginia, USA) in the shallow groove to separate the two tooth halves, one half

of each dentin surface was etched with phosphoric acid (K-etchant, Kuraray Noritake) for 15s. After rinsing with water spray, the separating razor blade was removed, upon which the whole dentin surface was gently air-dried. The four UAs investigated in this project part were the experimental two-step UA Exp_2UA, involving the application of G-PrBp as primer followed by the experimental adhesive resin BZF-21, the commercial UAs G-PrB, P&Ba and SBU, and the commercial two-step gold-standard SE adhesive CSE2, which was also used in a 3-step E&R mode.

Upon 1w water storage of the bonded specimens, per tooth 12 rectangular sticks (micro(μ)-specimens: 1×1 mm wide; 8-9 mm long) were prepared (as detailed in the Supporting Information). One third of the μ-specimens was tested immediately to measure the 'immediate' μTBS. Another one third of the μ-specimens was subjected to 6m water storage to measure the '6m-aged' μTBS. The remaining specimens were subjected to 1y water storage to measure the '1y-aged' μTBS. During storage, distilled water was changed every two weeks to accelerate μ-specimen aging. When specimens failed prior to actual testing, they were considered as pre-test failures (ptfs) and recorded as 0 MPa.[37] The detailed μTBS-test protocol was described in a previous study (see Supporting Information).[29]

Statistical analysis was performed with a linear mixed-effects model (LME; R3.1.0; R Foundation for Statistical Computing, Vienna, Austria) with specific contrasts. The data were analyzed for the three variables 'Adhesive' (G-PrBp+BZF-21, G-PrB, P&Ba, SBU and CSE2), 'Aging' (1w, 6m and 1y) and 'bonding mode' (E&R and SE). The significance level was set at $\alpha = 0.05$.

2.7. Fractographic analysis of failed μTBS specimens. Representative fractured surfaces of all experimental groups, concerning specimens that revealed a μTBS value around the mean or in case of ptf, were observed with scanning electron microscopy (SEM; JSM-6610LV, Jeol). SEM-specimen processing involved specimen fixation in 2.5% glutaraldehyde for at least 12h, gradual dehydration in ascending concentrations of ethanol solutions (25, 50, 75, and 95% for 30min, and 100% for 1h) and chemical drying with hexamethyldisilazane (HMDS; Acros Organics, Thermo Fisher Scientific, Geel, Belgium). The specimens were coated with gold using a gold-sputter coater (JFC-1300, Jeol), upon which SEM (JSM-6610LV, Jeol) photomicrographs were taken at 85-90×, 2000×, and 9000× (original) magnification at an operating voltage of 5 kV and a working distance of 10 mm.

2.8. Ultra-structural transmission electron microscopy (TEM) of the interface produced by the experimental two-step UA Exp_2UA and the reference adhesive CSE2 at dentin. Six (n=3 per adhesive) non-carious human third molars were prepared for TEM adhesive-dentin interfacial characterization. A standard bur-cut smear layer at mid-coronal dentin was produced as aforementioned. The experimental adhesive Exp_2UA and the commercial adhesive CSE2 were bonded to dentin in both E&R and SE modes using the same procedure as described to prepare the μTBS specimens. CSE2 is considered a gold-standard (two-step) SE adhesive, which was in this study also applied in an experimental three-step E&R bonding mode (application not recommended by its manufacturer). A thin 1-mm layer of the flowable composite G-ænial Universal Flo (GC) was applied on top and light cured for 20s using the LED light-curing unit Bluephase 20i (Ivoclar Vivadent) used in 'high mode'. The bonded specimens were stored for 24h in distilled water at 37°C. After sectioning the specimens in μ-specimens with 0.8-mm width using a water-cooled diamond saw (Accutom-50, Struers), half of the specimens were immediately processed for TEM, while the remaining specimens were subjected to 1y water storage. TEM-specimen preparation was processed as described in detail before,[38] including fixation in 2.5% glutaraldehyde for at least 12h, dehydration in ascending concentrations of ethanol solutions (25, 50, 75, 95 and 100%; immersion in each solution twice for 10min) and in 99% propylene oxide (Acros Organics, Thermo Fisher Scientific, Geel, Belgium) three times for 10min, and finally embedding in epoxy resin (Sigma-Aldrich Chemie, Steinheim, Germany), prior to being sectioned with an Ultra 45° (Diatome, Nidau, Switzerland) diamond knife in an Ultracut UCT (Leica) ultramicrotome to obtain ultra-thin 70- to 90-nm cross-sections for TEM examination (JEM-1200EX II, Jeol).

2.9. *In-situ* zymography of the interface produced by the experimental two-step UA Exp_2UA and the reference adhesive CSE2 at dentin. Eight (n=4 per adhesive) non-carious human third molars were prepared for zymographic adhesive-dentin interfacial analysis. The mid-coronal dentin surface was equally split into two parts by cutting a shallow groove of 0.3-mm width and 0.5-mm depth. A standard dentin smear layer at mid-coronal dentin was produced using 320-grit silicon-carbide paper (Hermes, Hamburg, Germany) for 30s. The tooth specimens were then sectioned parallel to the dentin surface to gain dentin disks with a 1-mm thickness. The experimental adhesive Exp_2UA and the commercial adhesive CSE2 were bonded to dentin in both E&R and SE mode using the same procedure as described to prepare the μTBS and TEM specimens. A thin 1-mm layer of the flowable composite G-ænial

Universal Flo (GC) was applied on top and light cured for 20s using the LED light-curing unit Bluephase 20i (Ivoclar Vivadent) used in 'high mode'. After bonding, the specimens were stored in distilled water at 4°C for 24h and then cut vertically to obtain 1-mm thick slabs using the Accutom-50 (Struers) diamond saw. Each slab was glued to a plexiglass slide and subsequently polished using P1200 and P4000 SiC paper (Struers) and polishing cloth paper (MicroCloth, PSA, Buehler, Lake Bluff, IL, USA) with 6- and 3-µm diamond suspensions (Kemet International, Maidestone, UK) using a grinding/polishing machine (Beta Grinder-Polisher, Buehler). The polishing process was finished when dentin tubules appeared transparent under 40×-magnification light microscopy (Axio Imager M2, Carl Zeiss Microscopy, Jena, Germany).

Dye-quenched (DQ)-gelatin (Invitrogen, Carlsbad, CA, USA), which consists of quenched FITC-labeled gelatin, was used as MMP substrate and was dissolved in water at 1 mg/ml.[39] The gelatin stock solution was 1:8 diluted with dilution buffer (50 mM Tris-HCl, 50 mM NaCl, 5 mM $CaCl_2$, pH 7.4). The adhesive-dentin interface was next demineralized with 1% phosphoric acid (Orthophosphoric acid 85%, AnalaR NORMAPUR, VWR International, Leuven, Belgium) for 10s and rinsed with distilled water for 1min, upon which 50 µl of gelatin mixture was added and covered with a glass coverslip. The specimens were kept overnight in a dark humid chamber at 37°C and examined using a confocal laser scanning microscope (CLSM; Leica TCS SP8X, Leica Microsystems, Wetzlar, Germany) with an excitation wavelength of 488 nm and emission wavelength of 530 nm. From every specimen, a series of two-dimensional images were captured at two central spots along the adhesive-dentin interface, starting at the specimen surface moving down below the surface into the specimen with successive Z-depth steps of 1 µm. Endogenous gelatinolytic enzyme activity appeared as green fluorescence. The images were processed using Fiji ImageJ (National Institutes of Health, Bethesda, Maryland, USA).

2.10. Anti-bacterial efficacy of the experimental adhesive resin BZF-21.

2.10.1. Bacterial growth spectrophotometry. Experimental BZF-21 adhesive disks with a 7-mm diameter and 2-mm thickness were made using silicone molds (Aquasil medium body, Dentsply Sirona) protected with a glass slide to avoid polymerization inhibition by oxygen. The adhesive disks were light cured at the center for 60s at both sides using the LED curing light Bluephase 20i (Ivoclar Vivadent) used in 'high mode'. The specimens were next cleaned ultrasonically in Milli-Q water for 15s, before they were sterilized with UV light for 6h. Four experimental BZF-21 adhesive-resin disks were placed

in wells of a 48-well plate and exposed to 300 µl of BHI solution for 24h. A total of 1200 µl extracted solution, in which the adhesive-resin disks were immersed for 24h, was collected.

Overnight cultures of *Streptococcus mutans* (*S. mutans*, ATCC 25175) were centrifuged and re-suspended in fresh Brain Heart Infusion broth (BHI, Becton Dickinson and Company, Franklin Lakes, NJ, USA).[40] *S. mutans* suspension (20 µl) with a concentration of 2×10^8 colony-forming units (CFU)/ml was added to the extracted solution (180 µl) in wells of a 96-well plate to obtain a final concentration of 2×10^7 CFU/ml. As positive and negative control, respectively, three wells received BHI supplemented with 2% glucose and another three wells received BHI supplemented with 2% penicillin, which inhibited *S. mutans* growth. All specimens with *S. mutans* cultures were incubated (37°C, 5% CO_2) under aerobic conditions. During 24h incubation, the optical density (OD) of bacterial suspensions was measured with 2h intervals at 630 nm and 37°C using a microplate reader (Multiskan Ascent,Thermo Fisher Scientific, Vantaa, Finland). The experiments were repeated 3 times independently.

2.10.2. *S. mutans* CFU counts on the experimental adhesive resin BZF-21. Fresh experimental BZF-21 adhesive (5 µl) was placed in wells of a 96-well plate and exposed to 200 µl of *S. mutans* suspension (2×10^7 CFU/ml). Wells that did not receive adhesive served as blank controls. After incubation at 37°C under aerobic conditions for 24h, 100 µl original bacterial suspension was added to 900 µl sterile physiological water (0.9% NaCl). The bacterial suspension was next ten-fold serially diluted, of which 50 µl was inoculated onto a blood agar plate using an automatic spiral inoculator (Spiral system, L.E.D. Techno, Heusden-Zolder, Belgium). The plate was cultivated at 37°C for 48h, upon which *S. mutans* colony-forming unit (CFU) counts were manually counted. The experiments were repeated 3 times. Data were expressed as $\log_{10}$ CFU/ml for BZF-21 and the control.

2.10.3. Biofilm structure on the experimental adhesive resin BZF-21 examined by SEM. Three experimental BZF-21 adhesive-resin disks were separately exposed to 2 ml of *S. mutans* suspension with 2% glucose in a 24-well plate. Part of disk surface that was not exposed to biofilms was marked by a thin razor blade (009 RD single edge carbon steel, American Safety Razor). After incubation at 37°C for 24h, adherent *S. mutans* biofilm development on the BZF-21 adhesive disks was observed using SEM (JSM-6610LV, Jeol). The disks with attached *S. mutans* were rinsed twice with sterile PBS and fixed in 2.5% glutaraldehyde for 2h, dehydrated in ascending concentrations of ethanol solutions

(50, 70 and 90% for 10min, and 100% three times for 15min) and chemically dried with hexamethyldisilazane (HMDS; Acros Organics). After that, the specimens were sputter-coated with gold using a gold-sputter coater (JFC-1300, Jeol) and observed by SEM (JSM-6610LV, Jeol) at an operating voltage of 5 kV and a working distance of 10 mm.

3. RESULTS

3.1. STEM/EDS of BZF-21. STEM in bright-field (BF) mode revealed that the zinc-calcium-fluoride glass filler within the experimental adhesive resin BZF-21 was irregular with an average filler size of about 250 nm (Figures 1a and 1b). STEM/EDS mapping identified the elemental composition of the glass filler with the main detected elements being Si and O. The presence of Zn, Ca and F within the adhesive was confirmed. In addition to the Zn-Ca-F glass filler, BZF-21 contains about 50-nm classic silica (SiO_2, Figure 1c). Furthermore, overview TEMs of the filler-matrix configuration within BZF-21 are presented in the Figure S1.

3.2. Ion release of BZF-21. The ions Zn, Ca and F were gradually released from the experimental adhesive resin BZF-21 (Figure 1d), with the highest ion release measured for Zn, then Ca and the least for F (Figure 1e). When the immersion solution was changed every week to avoid a saturation effect, the amount of Zn, Ca and F release was highest during the first day, followed by a relatively sharp decrease to a nearly constant level from the first week (Figure 1f).

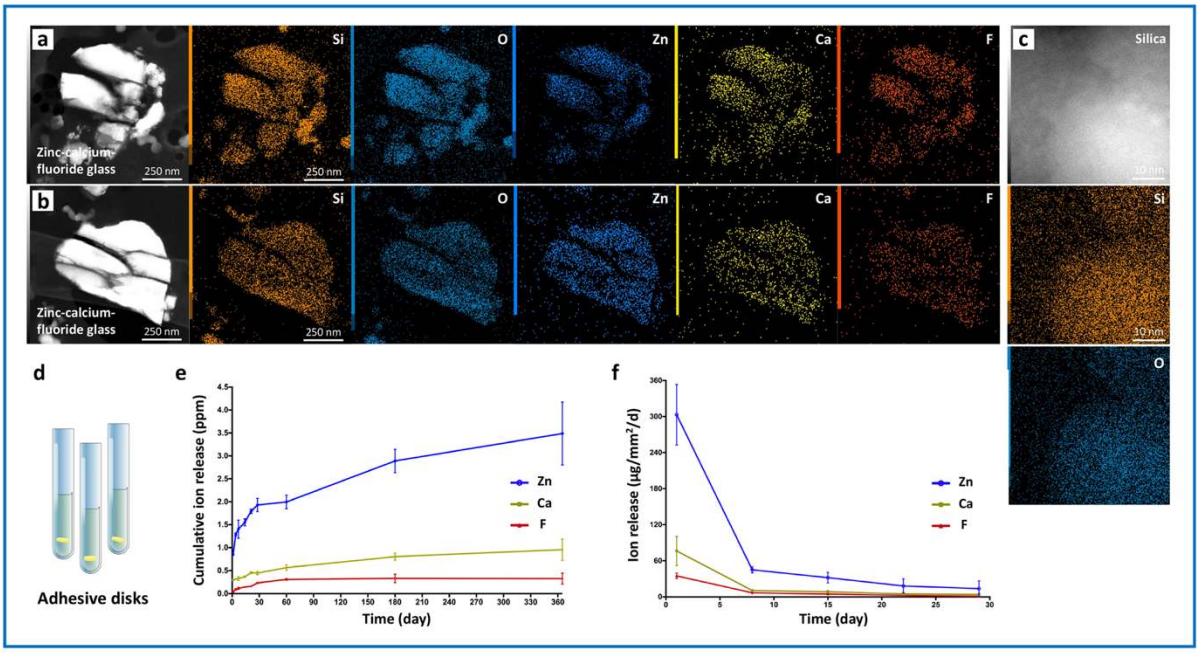

Figure 1. STEM/EDS of zinc-calcium-fluoride (Zn-Ca-F) bioglass incorporated into the experimental multi-functional adhesive resin BZF-21 **(a-c)** and ion release from the experimental adhesive resin BZF-21 in function of time, as measured by ICP-OES and a F ion-specific electrode **(d-f)**. Release kinetics of the ions Zn, Ca and F from the BZF-21 during a period of 1 year, with the highest cumulative ion release measured for Zn, then Ca and the least for F (Figure 1e). To avoid a saturation effect, the immersion solution Milli-Q water was changed every week (Figure 1f). Release kinetics of the ions Zn, Ca and F from the BZF-21 during a period of 28 days, with an initial high release of Zn, Ca and F over the first day (Figure 1f). Overview (S)TEMs illustrate the filler-matrix configuration of BZF-21 in the Figure S1.

3.3. Water sorption and solubility of BZF-21 and the reference adhesives. As pooled water sorption and solubility data (7d, 6m and 1y) of each experimental group did not reveal normal distribution but unequal variance, Kruskal Wallis non-parametric statistical analysis was applied to identify statistically significant differences. The lowest water sorption and solubility were observed for BZF-21 and the adhesive resin ('Bond') of CSE2 (Figure 2A,B). P&Ba revealed the highest water sorption and solubility, solely not being significantly different from SBU, for which some intermediary water sorption and solubility data were measured. No data were recorded for G-PrB, as adhesive disks could hardly be obtained as they easily broke after curing (Figure 2C). The water sorption of BZF-21 or CSE2 Bond after 6m was not significantly different from that after 7d, while slightly but statistically significantly higher water sorption was measured at 1y. Likewise, the 1y solubility of BZF-21 and CSE2 Bond was slightly

but significantly higher than the 6m solubility, but solubility overall remained low for BZF-21 and CSE2 Bond.

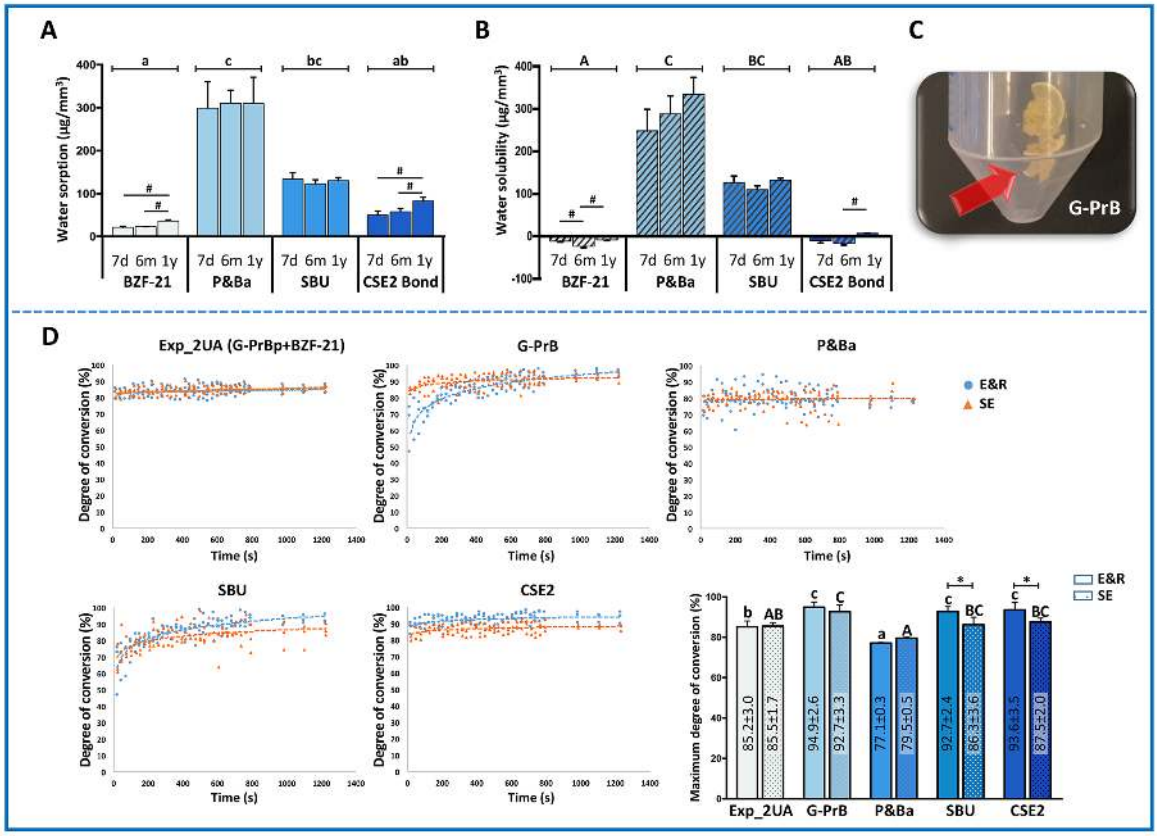

Figure 2. Water sorption **(A)** and solubility **(B)** (both in µg/mm^3) of the dental adhesives investigated after 7-day (7d), 6-month (6m) and 1-year (1y) water storage. The lowest water sorption and solubility were recorded for BZF-21 and the adhesive resin ('Bond') of CSE2 (Figure 2A,B). The same small or capital letters indicate absence of statistically significant difference ($p>0.05$). Columns distinguished with a hash key '#' are significantly different in pairwise comparisons ($p<0.05$). **(C)** Insufficiently polymerized fragment of G-PrB immersed in water, not allowing measurement of water sorption and solubility. Polymerization kinetics **(D)** with progression in degree of conversion (DC in %) upon application of the different adhesives to dentin in etch-and-rinse (E&R) and self-etch (SE) mode, as measured within the first 20min after application to achieve maximum DC, as was also graphically presented in the bar graph. In the latter graph, the same small or capital letters indicate absence of statistically significant difference ($p>0.05$).

3.4. DC of Exp_2UA and the reference adhesives. DC progression of the five dental adhesives for 20min, used either in SE or E&R mode, is graphically presented in Figure 2D. For polymerization-kinetics analysis, DC-progression curves were fitted to express DC in function of the log-transformed

time in s. The lowest (mean) 'initial' DC (20s after light curing) was 63.1% and 65%, as was recorded for G-PrB and SBU, respectively, when both adhesives were applied in E&R mode. All other adhesives revealed relatively higher initial DCs. Regarding 'maximum' DC, two-way ANOVA showed significant differences for the two factors 'adhesive' ($p<0.001$) and 'bonding mode' ($p=0.019$). The interaction between the two factors was also significant ($p=0.027$). For all adhesives, the (mean) maximum DC varied between 77.1% and 94.9% when the adhesives were used in E&R mode, and between 79.5% and 92.7% when used in SE mode. The lowest maximum DC was measured for P&Ba, being significantly lower than the respective maximum DCs measured of all other adhesives, except for Exp_2UA applied in SE mode. The highest maximum DCs were recorded for G-PrB, SBU and CSE2. Comparing E&R versus SE modes, only SBU_SE and CSE2_SE revealed significantly lower maximum DCs as compared to their SBU_ER and CSE2_ER counterparts, respectively. Regarding the two-step UA Exp_2UA, no significant difference in DC was found between Exp_2UA_ER (85.2 ± 3.0%) and Exp_2UA_SE (85.5 ± 1.7%).

3.5. μTBS to dentin of Exp_2UA and the reference adhesives. The μTBS data are graphically depicted in box plots in function of water storage (aging) when the adhesives were used in E&R and SE mode in Figures 3A and B, respectively. The μTBS data of the reference adhesive CSE2 with 95% confidence intervals were presented as grey background boxes. Overall, when applied both in E&R and SE mode, Exp_2UA produced the highest μTBSs that additionally reduced least upon aging among all adhesives investigated. More specifically, Exp_2UA's 1y-aged bond strength was significantly higher than those recorded for all other adhesives, except for a non-significantly different μTBS measured for CSE2 applied in SE mode and SBU used in E&R mode (Figure 3A). Used in SE mode, Exp_2UA's 1w-(immediate), 6m- and 1y-aged μTBSs were significantly higher than those recorded for all other adhesives, except for non-significantly different μTBSs measured for the reference adhesive CSE2 (Figure 3B). Comparing E&R versus SE bonding mode, the immediate 1w μTBS of all one-step UAs applied in SE mode was significantly lower than those recorded in E&R mode, except for Exp_2UA, for which similar μTBSs were recorded when used in E&R and SE bonding modes ($p>0.05$). One-year (1y) water-storage aging significantly decreased the μTBSs of all adhesives (compared with the 1w μTBS), regardless of if they were used in E&R or SE mode, except for Exp-2UA that withstood bond degradation when it was used in SE mode (no significant μTBS reduction) and solely a significantly

lower 1y μTBS was recorded when it was used in E&R mode (and except G-PrB used in SE mode that however already resulted in significantly lower 1w and 6m μTBSs).

3.6. Fractographic analysis of failed μTBS specimens. Representative SEM photomicrographs of fractured Exp_2UA μ-specimens (dentin side, 9000× original magnification) upon 1w and 1y water-storage aging when the adhesive was used in E&R and SE mode are presented in Figure 3C, while SEM photomicrographs of SBU groups used in E&R and SE mode upon 1w and 6m water storage are shown in Figure 3D.

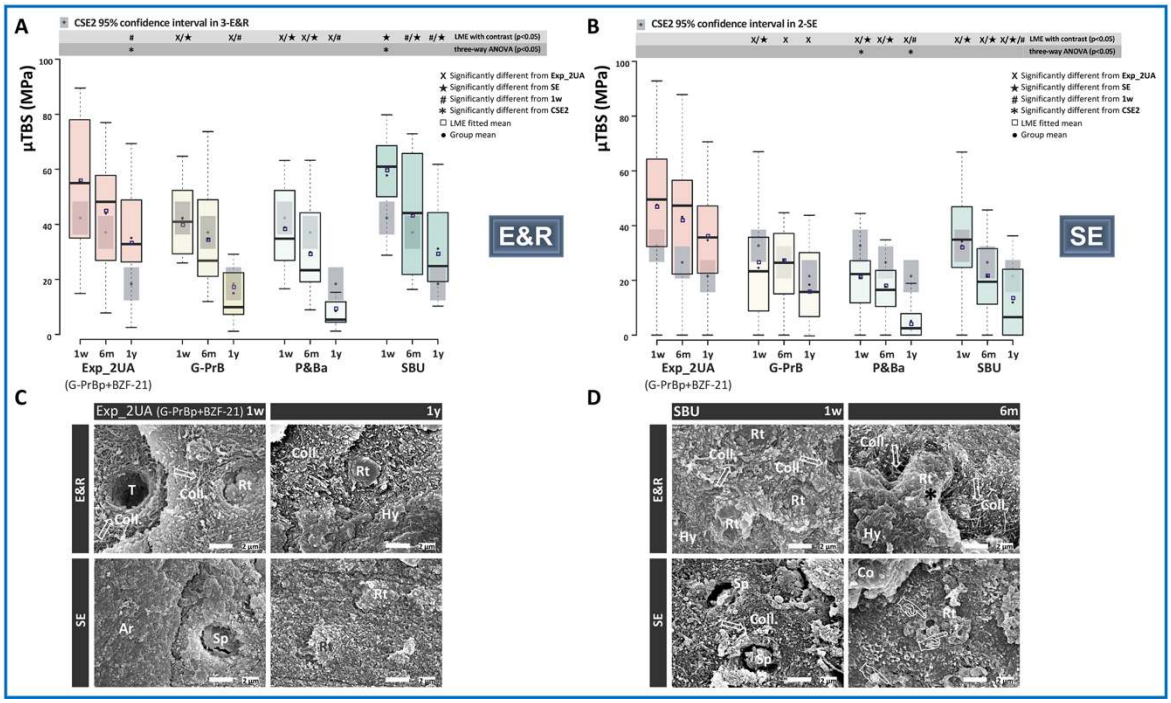

Figure 3. Box-and-whisker plot graphs of 'immediate' μTBS (in MPa), which was measured upon 1w water storage, and 'aged' μTBS, which was measured after 6m and 1y water storage, for the experimental multi-functional adhesive Exp_2UA and the reference UA adhesives (G-PrB: G-Premio Bond, GC; P&Ba: Prime&Bond Active, Dentsply Sirona; SBU: Scotchbond Universal, 3M Oral Care) investigated when they were used in E&R **(A)** and SE **(B)** bonding mode. The grey boxes in the background represent the 95% confidence interval of the reference adhesive Clearfil SE Bond 2 (CSE2; Kuraray Noritake). Statistically significant differences are presented using specific symbols. Representative SEM photomicrographs in high magnification (9000× original magnification) of the 'immediate' (1w) and 'aged' (1y) fractured μTBS micro-specimens of the experimental adhesive Exp_2UA **(C)**, and the 'immediate' (1w) and 'aged' (6m) fractured μTBS micro-specimens of SBU **(D)**. Ar: Adhesive resin; Coll.: Collagen fibrils; Hy: Hybrid layer: Rt: Resin tag; Sp: Smear plug; T: Tubule.

3.7. TEM of the interface produced by Exp_2UA and the reference adhesive CSE2 at dentin. The immediate (1w) adhesive-dentin interfacial ultra-structure produced by Exp_2UA applied in E&R mode (Figure 4a-c) differs from when applied in SE mode (Figure 4d-f). Both interfacial ultra-structures revealed an about 20-µm thick adhesive-resin layer, which was homogeneously filled with zinc-calcium-fluoride glass and silica (SiO_2) filler particles. When used both in E&R and SE bonding mode, Exp_2UA bonded tightly to dentin without any interfacial separation noted. When Exp_2UA was applied in E&R mode, phosphoric-acid etching resulted in relatively deep demineralization of dentin and upon subsequent resin infiltration in a relatively thick (5-6 µm) hybrid layer, in which all hydroxyapatite was dissolved and removed by the E&R process (Figure 4a-c). No interfacial smear debris from surface preparation by bur remained, while the dentin tubules were opened and allowed resin tags to have been formed. When Exp_2UA was applied in SE mode, the dentin surface was solely shallowly and partially demineralized, having resulted in a relatively thin (about 200 nm to submicron) hybrid layer (Figure 4d-f). Higher magnification (150,000× original magnification) disclosed morphological features compatible with 10-MDP_Ca-salt nano-layering within the adhesive-resin layer near the hybrid layer (Figure 4e,f).

One-year (1y) water-storage aging of specimens did not result in ultra-structurally different interfacial features of Exp_2UA bonded in E&R and SE bonding mode (Figure 5). No ultra-structural indications of bond degradation were detected. Even more, after 1y aging morphological features compatible with 4-nm 10-MDP_Ca-salt nano-layering could still be found for both bonding modes (200,000× original magnification).

As reference, CSE2 applied in the experimental E&R mode, including beforehand phosphoric-acid etching, revealed a hydroxyapatite-free and collagen-rich 2- to 4-µm thick hybrid layer and evident resin tags (Figure 6a,b). Applied in SE mode, a typical hydroxyapatite-rich submicron hybrid layer was formed (Figure 6c,d). Low-magnification (10,000× original magnification) TEM revealed that the thickness of the adhesive-resin layer was approximately 5-6 µm, being much thinner than that of Exp_2UA (ca. 20 µm). After 1y water-storage aging, no ultra-structural interfacial difference was observed with the exception of evident de-bonding of filler particles from the adhesive-resin layer of CSE2 when used both in E&R and SE bonding mode, leaving some voids (Figure 6e-h).

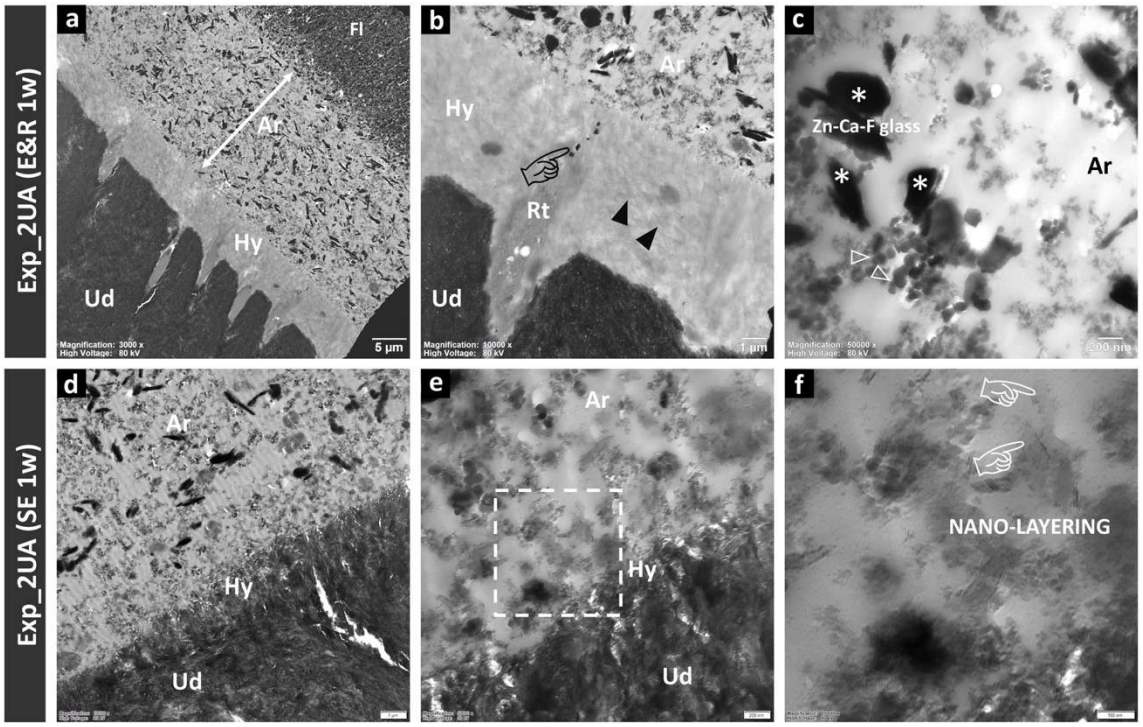

Figure 4. Ultra-structural TEM photomicrographs of the adhesive-dentin interface produced by Exp_2UA when applied in E&R **(a-c)** and SE **(d-f)** bonding modes upon 1w water storage. Overview of the interface when Exp_2UA was applied in E&R mode **(a)**, revealing a tight adhesive-dentin interface with a thick adhesive-resin layer (Ar) of approximately 20 µm. Higher magnification of (a) presents in **(b)** a dentinal tubule, which was filled with adhesive resin, having formed a resin tag (Rt). Black handpointer: filler particles originated from the adhesive resin. Black closed arrowhead: collagen fibrils being observed as electron-lucent structures as the sections were not stained with heavy metals. Higher magnification of the zinc-calcium-fluoride glass filler within the adhesive resin BZF-21 **(c)**. Asterisks: highly dispersed Zn-Ca-F glass. White open arrowheads: silica (SiO_2) filler particles. Overview of the adhesive-dentin interface produced by Exp_2UA when applied in SE mode, revealing a thin hybrid layer (Hy) of less than 1-µm thickness **(d)**. Higher magnification of Exp_2UA's SE adhesive interface **(e).** Higher magnification of the white square in (e) discloses in **(f)** 'nano-layering' structures (white handpointers) immediately adjacent the hybrid layer and spread within the adhesive-resin layer. Ar: adhesive resin; Fl: flowable composite; Hy: hybrid layer; Rt: resin tag; Ud: unaffected dentin.

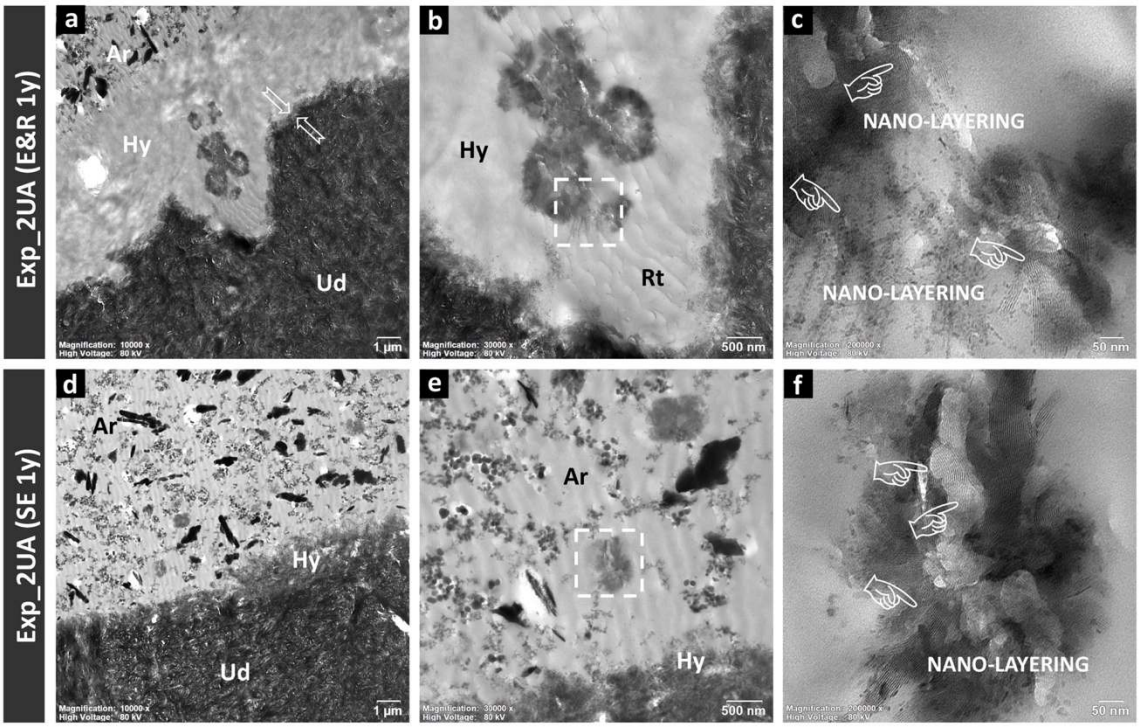

Figure 5. Ultra-structural TEM photomicrographs of the adhesive-dentin interface produced by Exp_2UA when applied in E&R **(a-c)** and SE **(d-f)** bonding modes upon 1y water storage. Overview of Exp_2UA's adhesive-dentin interface when Exp_2UA was applied in E&R mode **(a)**. While all mineral is dissolved/removed within the hybrid layer (Hy) body, a solely partially demineralized zone with a thickness of around 500 nm (between open arrows) was detected above the transition of the hybrid layer to unaffected dentin (Ud). Multiple nano-layering clusters were detected within the adhesive-resin layer **(b).** These nano-layering structures (white handpointers) resisted 1y water-storage degradation **(c)**. Overview of Exp_2UA's adhesive-dentin interface when Exp_2UA was applied in SE mode **(d)**. Higher magnification of Exp_2UA's SE adhesive interface **(e)**. The observed nano-layering (white handpointers) typically revealed a periodicity of ca. 4 nm **(f)**. Ar: adhesive resin; Hy: hybrid layer; Ud: unaffected dentin.

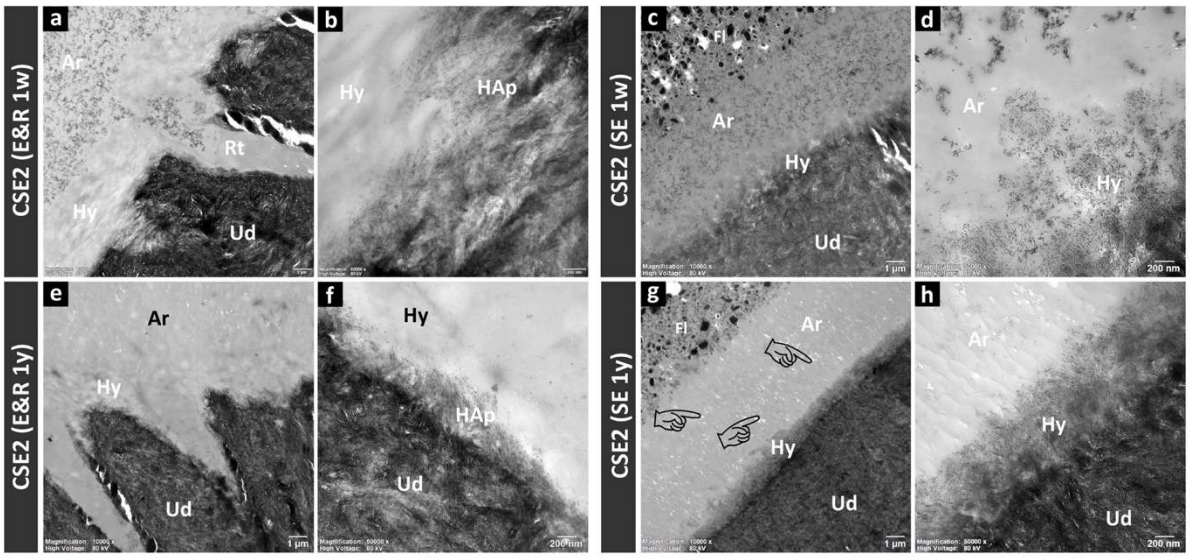

Figure 6. Ultra-structural TEM photomicrographs of the adhesive-dentin interface produced by CSE2 when it was applied in E&R (a,b and e,f) and SE (c,d and g,h) modes upon 1w (a-d) and 1y (e-h) water storage. Overview of the adhesive-dentin interface when CSE2 was applied in E&R bonding mode upon 1w water storage **(a)**. Higher magnification of CSE2's E&R adhesive interface **(b)**. A gradual transition with a solely partially demineralized zone was observed at the hybrid layer (Hy) bottom. Overview of the adhesive-dentin interface when CSE2 was applied in SE mode upon 1w water storage, revealing a tight adhesive-dentin interface, presenting with an adhesive-resin (Ar) layer of ca. 5-6 µm thickness **(c)**. Higher magnification of CSE2's SE adhesive interface **(d)**. Overview of CSE2's E&R adhesive interface upon 1y water storage, disclosing filler de-bonding within the adhesive resin **(e)**. Higher magnification of CSE2's E&R adhesive interface **(f)**. Overview of CSE2's SE adhesive interface upon 1y water storage, revealing filler de-bonding within the whole adhesive layer and hereby having left interfacial porosities (black handpointers) as indications of hydrolytic bond-degradation effects **(g)**. Higher magnification of CSE2's SE adhesive interface **(h)**. Ar: adhesive resin; Fl: flowable composite; Hy: hybrid layer; Rt: resin tag; Ud: unaffected dentin.

3.8. *In-situ* zymography of the interface produced by Exp_2UA and the reference adhesive CSE2 at dentin. Qualitative analysis of interfacial green fluorescence-signal intensity revealed a higher fluorescence intensity when Exp_2UA and CSE2 were used in E&R than in SE bonding mode (Table 1). No distinct difference was detected between Exp_2UA and CSE2. For 75% of the Exp_2UA specimens bonded in E&R mode, *in-situ* zymography revealed green fluorescence within the hybrid layer (especially at the bottom of hybrid layer), indicating that the fluorescein-conjugated gelatin was

hydrolyzed at these spots. For 50% Exp_2UA specimens bonded in SE mode, no fluorescence was detected at the adhesive-dentin interface.

Representative CLSM images of the adhesive-dentin interfaces produced by Exp_2UA and the reference adhesive CSE2 at dentin are presented in Figure 7. Clearly more intense fluorescence was detected within the hybrid layer, especially at the hybrid-layer bottom, and at the resin tags when both adhesives were used in E&R than in SE bonding mode.

Table 1 Qualitative analysis of green fluorescence-signal intensity at the adhesive-dentin interface for Exp_2UA and the reference adhesive CSE2.

Exp_2UA	E&R		SE		CSE2	E&R		SE	
	Spot 1	Spot 2	Spot 1	Spot 2		Spot 1	Spot 2	Spot 1	Spot 2
Tooth 1	++	++	+	+	Tooth 5	++	+	+	+
Tooth 2	-	-	++	+	Tooth 6	+	+	+	-
Tooth 3	+	+	-	-	Tooth 7	++	++	+	+
Tooth 4	+	+	-	-	Tooth 8	-	-	-	-
SUM*	6		1			7		2	

'++': strong fluorescence signal (= 2); '+': weak fluorescence signal (= 1); '-': no fluorescence signal (= -1); SUM = Sum of figures allocated to the plusses and minuses.

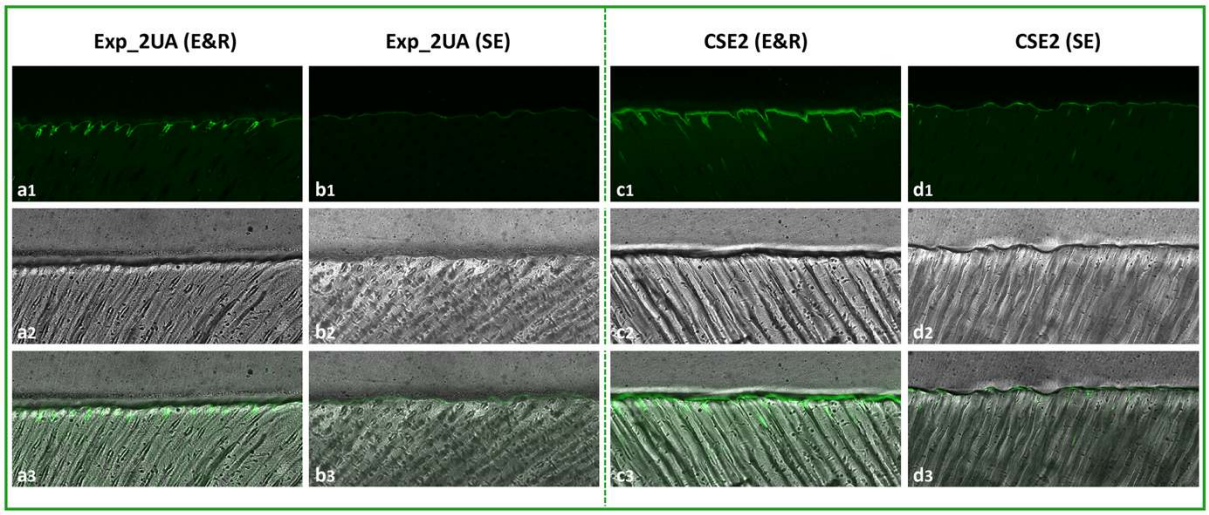

Figure 7. *In-situ* zymography to evaluate the anti-enzymatic properties of Exp_2UA and CSE2. Representative CLSM photomicrographs of proteolytic activity within the hybrid layer and resin tags of adhesive-dentin interfaces produced by Exp_2UA (a1-a3, b1-b3) and CSE2 (c1-c3, d1-d3), when both adhesives were applied in E&R (a1-a3, c1-c3) and SE (b1-b3, d1-d3) bonding modes. Green fluorescence **(a-d1)** indicates that the fluorescein-conjugated gelatin was hydrolyzed and endogenous proteolytic activity

was detected. Differential interference contrast images of the respective adhesive-dentin interfaces **(a-d2)**. Merged images of (a-d1) and (a-d2) are presented in **(a-d3)**.

3.9. Anti-bacterial efficacy of BZF-21. The growth of *S. mutans* in the extract from the experimental BZF-21 adhesive-resin disks (Figure 8A) appeared not inhibited. Optical density (OD) of BZF-21 after 24h was similar to that of BHI (no BZF-21) and significantly higher than that of the negative control, containing 2% penicillin as antibiotic (Figure 8B,C). However, CFU counts revealed significantly lower *S. mutans* colonies growing on fresh experimental BZF-21 as compared to the blank control group (Figure 8D).

Representative SEM photomicrographs of *S. mutans* biofilm grown on BZF-21 adhesive-resin disks are presented in Figure 8E. Higher magnification confirmed adherence of *S. mutans* with intact bacterial structure to the adhesive surface.

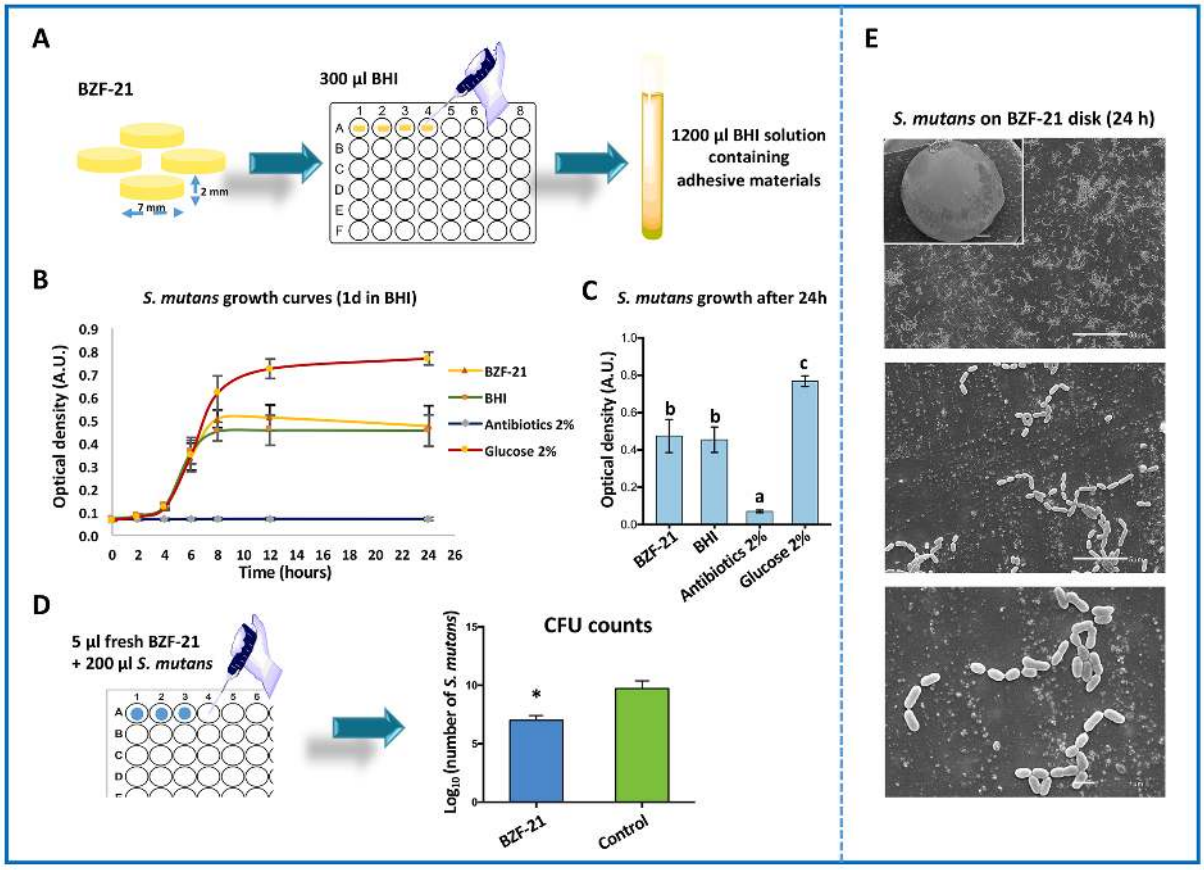

Figure 8. Anti-bacterial properties of the experimental adhesive resin BZF-21. Collection of solutions extracted from experimental BZF-21 adhesive-resin disks **(A)**. *S. mutans* growth measured spectrophotometrically (OD: optical density) in function of time **(B)** and after 24h incubation **(C)**. The data are presented as mean ± standard deviation. The same letters indicate absence of statistically significant

differences ($p>0.05$). Colony-forming unit (CFU) counts of fresh adhesive resin BZF-21 versus that of a blank control **(D)**. Statistically significant difference was indicated by the asterisk. Representative SEM photomicrographs of biofilm formation of *S. mutans* on experimental adhesive BZF-21 disks **(E)**.

4. DISCUSSION

UAs applicable in both E&R and SE mode following a two-step application procedure rarely exist today. The adhesive designed and developed in this work combines a primer, containing 10-MDP as the currently most effective functional monomer possessing chemical binding potential to hydroxyapatite, with a bioglass-containing hydrophobic adhesive resin. The rationale behind this development is to compensate for the inherent high hydrophilicity of current UAs by the extra hydrophobic resin layer in order to better protect the adhesive interface against hydrolytic aging. At the same time, Exp_2UA provides a thicker film thickness with enhanced stress-absorbing potential. Besides intending to increase the hydrophobic nature of the adhesive-dentin interface with this innovative two-step UA, active bioglass filler was added to the adhesive formulation to render the adhesive additional anti-enzymatic/bacterial bio-functions.

STEM/EDS and ion-release experiments confirmed that the bioactive filler particles incorporated into the experimental adhesive resin BZF-21 gradually released Zn, Ca and F ions despite being polymerized. Zn release was higher than the release of Ca and F, with ion release being detected over one year. After an initial burst release in the first week, the ion-release rate decreased over time, which should be attributed to a saturation or concentration-gradient effect.[41] Initially, ions in direct contact with water at the adhesive-disk surface were readily released. After 1 week or a longer time period, a concentration gradient of ions was created in the adjacent water environment, by which ions inside the adhesive were more difficultly released.

Most convincing data indicating that a more hydrophobic adhesive-dentin interface can be achieved with Exp_2UA, were the extremely low water sorption and solubility recorded for BZF-21. In fact, the lowest water sorption and solubility were found for the experimental adhesive resin BZF-21, scoring even slightly, but not statistically significantly better than the commercial adhesive resin CSE2 Bond. Both BZF-21 and CSE2 Bond are definitely more hydrophobic and absorb less water than the reference UAs, with SBU revealing an intermediary degree of water sorption and solubility. Different

material factors co-determine water sorption and solubility, as there are in the first place the kind/amount of mono/bi-functional monomers with potential hydrophilic monomer parts/ends, and also the kind/amount of cross-linking monomers, filler, solvents and other adhesive components (e.g. photo-initiator). The experimental adhesive resin BZF-21 solely contains di-methacrylate cross-linking monomers and does not contain HEMA nor 10-MDP. HEMA's hydroxyl group and 10-MDP's phosphate group will otherwise attract water, known to cause plasticization and deterioration of the mechanical properties of the polymer matrix.[42] In addition, the experimental adhesive contains relatively (for an adhesive resin) large sizes of bioactive glass (ca. 250 nm) in addition to classic silica (ca. 50 nm). Also other particle-filled adhesives presented lower water sorption than unfilled ones.[32,43]

The highest water sorption and solubility measured for P&Ba, although it does also not contain the highly hydrophilic monomer HEMA, confirms the excellent wetting behavior and the by-the-manufacturer claimed 'active moisture control with reliable performance on over-wet and over-dried dentin'.[44] However, the downside is the expected higher sensitivity for hydrolytic bond degradation through enhanced water sorption.[45-46] In contrast to BZF-21, P&Ba does also not contain inorganic filler particles.[42] Worth noting is that the water sorption and solubility of the UA G-PrB could not be measured; sufficiently polymerized adhesive disks could not be prepared, which should be attributed to its high amount of acetone solvent (25-50%). The present results demonstrated that P&Ba and SBU absorbed most water within the first week of water storage. No significant difference in water sorption was found between the immediate 1w and aged 1y data. Although still being low, the more hydrophobic adhesive resins BZF-21 and CSE2 Bond revealed their maximum water uptake after 1y water storage. The slow but continued water sorption of BZF-21 and CSE2 Bond over a long time period of one year indicates that the two adhesives must have formed denser polymer networks that resist water uptake. Surprisingly, BZF-21 and CSE2 Bond showed negative data for water solubility. Nevertheless, this result does not mean that the two adhesive resins did not dissolve into water. Previously absorbed water might have turned into 'bound water'[42] within the material, which cannot be released back into the solution medium.[47]

Above all, the first null hypothesis tested that water sorption and solubility of the new multi-functional adhesive was at least statistically equivalent to those of the reference adhesives, failed to be rejected. Further studies should also measure a mixture of primer and adhesive resin for two-step adhesives, hereby more closely mimicking the application protocol clinically executed.

An often underestimated factor co-determining bonding effectiveness is polymerization efficiency. DC was measured using micro-Raman spectroscopy by focusing the 785-nm laser on the adhesive-covered dentin disks. As the laser was focused through a 50 × 1000-µm aperture in slit mode, the laser beam was strong enough to penetrate into the surface up to the deeper specimen layers. Hence, DC was measured based on spectra acquired from an area including the adhesive and hybrid layer, as well as the fully (E&R)/partially (SE) demineralized dentin, explaining the difference in DC depending if the adhesive was applied in E&R or SE mode.

Incomplete polymerization of the adhesive can accelerate bond degradation.[48] Camphorquinone (CQ) together with tertiary amine and diphenyl (2,4,6-trimethylbenzoyl) phosphine oxide (TPO) are the most widely used photo-initiators in contemporary dental adhesives.[36] The experimental adhesive resin BZF-21 combines the photo-initiator systems CQ/amine and TPO. In the present study, DC of all adhesives, regardless of bonding mode, increased with time (20min) to reach maximum DC. Although maximum DC of Exp_UA, applied in E&R mode (85.5%), was significantly lower than that of G-PrB (92.7%), initial DC (20s after light curing) of Exp_UA, applied in E&R mode (82.3%), was higher than that of G-PrB (63.1%), indicating that Exp_UA initially cured faster. This finding corroborated previous research that demonstrated that a TPO-based adhesive polymerizes much faster, while a solely CQ/amine-based adhesive possesses more dark cure to obtain a higher final DC.[36] Interestingly, the CQ/amine-based CSE2 showed an initial faster conversion rate (87.1%), which may be attributed to new 'integrated photo-initiators', as claimed by its manufacturer.[49] According to technical product information, these new initiators can generate more radicals upon light irradiation than conventional initiators.[49] Indeed, recent research found that the new photo-initiator added to the adhesive resin CSE2 Bond increased DC as compared to its predecessor Clearfil SE Bond.[50] In summary, BZF-21, combining the CQ/amine photo-initiator system with a TPO co-initiator, and CSE2 Bond, containing new 'integrated photo-initiators', polymerized faster than the three reference UAs investigated in this study.

Regarding bonding mode, no difference in DC was obtained when Exp_UA and P&Ba were used in E&R or SE bonding mode. G-PrB's DC was initially lower when used in E&R than SE mode, but eventually reached a higher final DC when G-PrB was used in E&R mode. A significantly higher DC was reached for SBU and CSE2 when used in E&R than in SE bonding mode over nearly the full measurement period. These differences in DC kinetics are indicative of material-specific properties. Overall, Exp_2UA

revealed polymerization kinetics and achieved maximum DC in line with those recorded for the reference adhesives, by which the second null hypothesis tested that polymerization efficiency of the new multi-functional adhesive was at least statistically equivalent to those of the reference adhesives, failed to be rejected.

An essential test for a new adhesive is to evaluate its immediate and aged bonding efficacy to dentin,[8,51] because bonding is the prime function of a dental adhesive. In this study, the new experimental adhesive Exp_2UA scored an overall superior bonding performance in both bonding modes than the other representative commercial UAs investigated. Noteworthy is that Exp_2UA continuously released ions without compromising its bonding effectiveness. Some bond degradation upon long-term water storage was recorded, but Exp_2UA withstood bond degradation best from all adhesives investigated in this study. Notably, also a consistently higher but mostly non-significantly higher bond strength was recorded for Exp_2UA compared with the considered gold-standard (SE) adhesive CSE2, with even the 1y-aged bond strength of Exp_2UA applied in E&R mode being statistically significantly higher than that of CSE2 applied in an experimental E&R bonding mode. This superior bond-strength performance of Exp_2UA should most likely be attributed to the following reasons differentiating Exp_2UA from the reference adhesives. First, TEM interfacial characterization of Exp-2UA revealed a dense and thick adhesive layer of nearly 20 µm, while the adhesive-layer thickness of all other adhesives investigated was below 10 µm, in this study shown for CSE2 by TEM but also observed for G-PrB [unpublished observation]; other studies revealed thin adhesive-resin layers for P&Ba[44] and SBU[52]. The thick adhesive-resin layer of highly hydrophobic nature better stabilizes, protects and seals the adhesive interface of Exp_2UA against water uptake and subsequent hydrolysis effects that can be considered to constitute the main bond-degradation mechanism. In addition, other studies have before shown that a uniform and thick adhesive resin can act as an intermediary stress reliever; such shock-absorbing potential can for instance better withstand polymerization shrinkage of the restorative composite applied on top, this especially in high C-factor cavity configurations in which high shrinkage stress is subjected to the adhesive interface.[53-54] Exp_2UA results in a relatively thick and hydrophobic adhesive-resin layer, as is also obtained with Optibond FL (Kerr). While not resulting in such a thick adhesive-resin layer as Exp_2UA, also CSE2's adhesive resin is of high hydrophobic nature, as evidenced by the low water sorption and solubility data generated in this study. In addition, containing today's most effective functional monomer 10-MDP, Exp_2UA's SE

bonding mechanism closely resembles that of CSE2. However, as reported earlier for CSE2's predecessor (Kuraray Noritake),[55] silica-filler de-bonding was also observed in this study for CSE2 when applied both in E&R and SE approach. This finding may actually explain CSE2's recorded lower aged bond strength as compared to that of Exp_2UA. This filler debonding is indicative of hydrolytic degradation of the filler-resin coupling in the adhesive resin. No signs of hydrolytic degradation of Exp_2UA's adhesive resin were ultra-morphologically observed by TEM in this study. Altogether, the third null hypothesis that the 'immediate' and 'aged' bonding efficacy to dentin of the new multi-functional adhesive did not significantly underscore those obtained by the reference adhesives, failed to be rejected.

Comparing the E&R and SE bonding modes of Exp_2UA, no statistically significant reduction in μTBS was found upon 1y water-storage aging when Exp-2UA was applied in SE mode as compared to Exp-2UA's immediate SE μTBS, while the 1y-aged μTBS significantly decreased when Exp_2UA was applied in E&R mode. These data confirm that SE bonding that combines micro-mechanical interlocking with additional chemical binding, achieves more stable bonding to dentin, as has repeatedly been documented before.[3-4] TEM interfacial characterization showed that Exp_2UA even produced 10-MDP_Ca nano-layering. These nano-layers have been identified to represent stable structures formed at adhesive-dentin interface that are thought to better withstand bond aging, hereby thus contributing to bond durability.[4,56-57] Overall, the unaltered interfacial ultra-structure observed upon long-term 1y water-storage complemented the stable bond-strength data measured for Exp_2UA. The significantly reduced 1y-aged bond strength, recorded when Exp_2UA was applied in E&R mode, must most likely be ascribed to degradation of collagen fibrils that were imperfectly encapsulated by resin, this particularly at the bottom of the thick E&R hybrid layer produced by Exp_2UA. SEM fracture analysis actually revealed indications of incomplete saturation of exposed collagen fibrils underneath Exp_2UA's E&R hybrid layer upon 1y aging.

Previous research has proposed several strategies to prevent and counteract adhesive-dentin bond degradation.[4,12] One considered effective and clinically practical bond-degradation-retarding strategy involves coating the interface with an extra hydrophobic resin to limit water uptake.[4,8,10] Primarily based on this strategy, Exp_2UA was designed, as this adhesive is to be applied in two steps with the final step involving the application of a hydrophobic adhesive-resin layer with a relatively thick film thickness.

Another commonly employed bond-degradation retarding strategy involves inhibition of enzymatic biodegradation or dentin bio-modification by collagen cross-linking.[4,19] Enzymes were shown to degrade collagen when they were exposed and insufficiently encapsulated by resin during hybridization.[16,18] MMPs belong to the zinc-activated and calcium-dependent endopeptidases.[58] A way to activate the enzymes is to disrupt the cysteine-zinc interaction by inducing conformation changes or by modifying or removing the propeptide domain.[59] Subsequently, the exposed Zn^{2+}-ion in the active site will bind a water molecule, by which the enzyme is activated and ready to cleave peptide bonds within proteins.[60] Thus, protein-protein interactions are to some extent controlled by the zinc-binding site. Previous research demonstrated that excess Zn can reduce MMP-mediated collagen degradation by acting as a competitive inhibitor of MMPs.[23] Additionally, Zn-doped bioglass filler has before been added to resin-based dental materials and evaluated on its remineralization and MMP-inhibition potential.[61-62] In the present work, Zn-Ca-F bioactive glass was incorporated into the experimental adhesive. *In-situ* zymography with CLSM was used to investigate the potential inhibitory effect of the experimental adhesive resin BZF-21. The results showed that for half of specimens bonded with Exp_2UA in SE mode, no fluorescence was detected at the adhesive-dentin interface. However, more than half of specimens (75%) bonded with Exp_2UA in E&R mode revealed a green fluorescence within the hybrid layer, demonstrating that the fluorescein-conjugated gelatin was hydrolyzed. Although less or weaker fluorescence signals were detected for the experimental adhesive as compared with that recorded for the reference adhesive CSE2, *in-situ* zymography suggested that enzymatic breakdown of the hybrid layer still occurred. This finding revealed that the experimental adhesive induced lower enzymatic activity, which may in part be related to Zn-ion release, but also that the enzyme-inhibiting effect was not that strong. Therefore, the fourth null hypothesis that the new multi-functional adhesive possessed anti-MMP bioactive potential, failed to be rejected.

Furthermore, our *in-situ* zymography data showed that the green fluorescence signals at interfaces originating from different young teeth (patient's age between 18 and 25 years) varied widely, indicating that *in-situ* zymography data should be interpreted with care regarding data representativeness, reliability and reproducibility. Very noteworthy is that previous research also pointed out that endogenic enzymes in teeth decrease with age and gradually disappear before the age of 40.[63] Hence, the involvement of enzymes in bond-degradation processes may clinically be much less determining as now abundant concerning literature seems to suggest.

Finally, the anti-bacterial effect of adhesive-disk extracts and fresh adhesive was investigated. Previous research indeed revealed that conventional composites lack the capacity to increase the local pH, which results in the outgrowth of more acidogenic/aciduric bacteria and stronger cariogenicity of the biofilm. Combined with absent antibacterial properties, lack of buffering may be obligated to the higher susceptibility of composites to secondary caries.[64] Therefore, dental adhesives with anti-microbial potential for preventing new caries development around composite restorations remain highly wanted.[26,65] *S. mutans* is the major cariogenic oral micro-organism causing caries.[66] Hence, in order to evaluate the anti-bacterial potential of Exp-2UA, we investigated *S. mutans* growth by OD and CFU, and examined its biofilm formation on adhesive disks. Results of this study presented that the polymerized adhesive disks did not inhibit growth of *S. mutans*, while also bacteria with a nearly completely intact morphology were observed by SEM to be attached onto the adhesive-disk surfaces. However, CFU data revealed that fresh BZF-21 significantly lowered *S. mutans* colonies compared with the control group, indicating that the growth of *S. mutans* was stopped or blocked because of the fresh adhesive resin. Zinc and fluoride are known to possess effective anti-bacterial effects.[28,67] Although the precise mechanism rendering fresh experimental BZF-21 anti-bacterial effects is still unclear, the enhanced release of Zn and F from the bioactive glass in an acidic environment is most likely involved.[68] Probably the released ions reacted with the surrounding medium of *S. mutans.* Another plausible anti-bacterial mechanism should be ascribed to BZF-21's relatively high pH of 8.2. Previous research found that *S. mutans* grown under pH-5.5 conditions revealed increased glycolytic activity than in a pH-6.5 environment.[69] Therefore, the high pH of the fresh experimental adhesive BZF-21 may have affected the metabolism of *S. mutans*. Given that fresh BZF-21 induced a moderate anti-bacterial effect, the fifth and last null hypotheses tested that the new multi-functional adhesive possessed anti-bacterial bioactive potential, also failed to be rejected.

In summary and schematically illustrated in Figure 9, application of Exp-2UA in both E&R and SE mode resulted in durable bonding performance to dentin, as evidenced by favorable 1y-aged bond-strength data and a tight interfacial ultra-structure that, as examined by TEM, remained ultra-morphologically unaltered upon 1y water-storage aging.

5. CONCLUSION

Responding to the research-and-development (R&D) intention to design and develop innovative dental adhesives that counteract interfacial bond degradation, we demonstrated with the present study that the experimentally developed adhesive is a promising candidate to combine high bonding potential and bond-degradation resistance through reduced water uptake, with anti-enzymatic and anti-bacterial therapeutic effects through gradual ion release from the contained bioactive zinc-calcium-fluoride bioglass. This innovative multi-functional adhesive with thick adhesive-resin film thickness enables a promising two-step universal approach (applicable in both E&R and SE bonding mode) to achieve longer lasting tooth restorations.

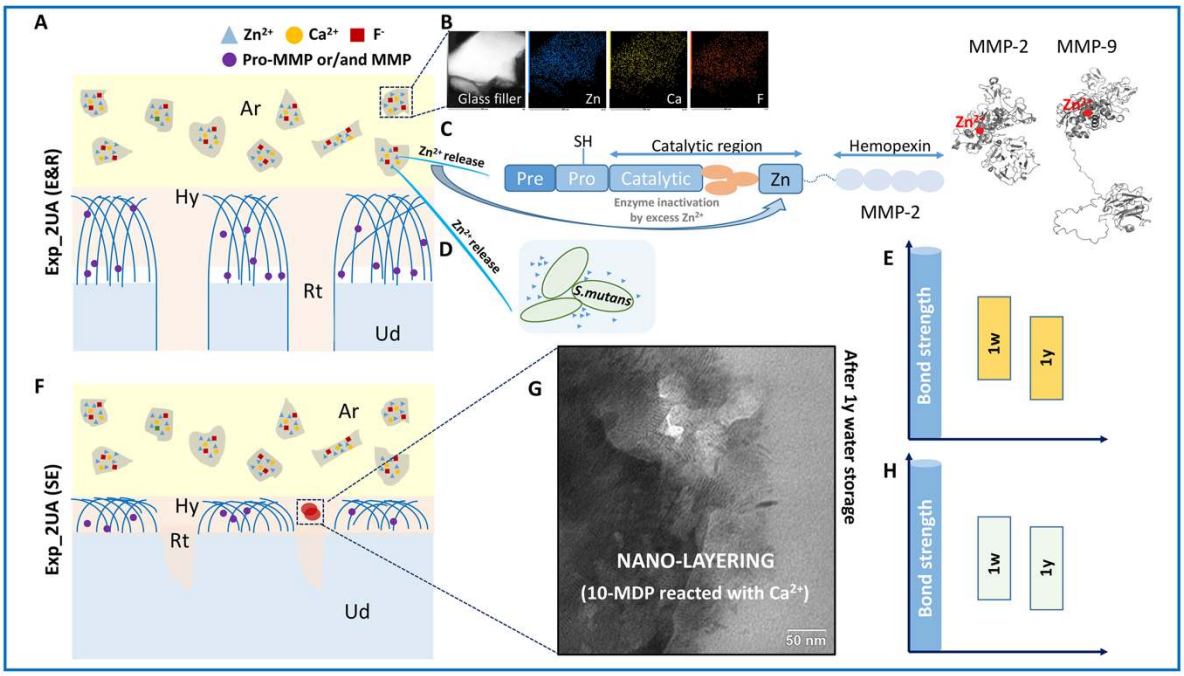

Figure 9. Collage illustrating the bonding efficacy, potential anti-MMP and anti-bacterial effect of the experimental multi-functional adhesive Exp_2UA. Schematic detailing the interfacial ultra-structure resulting when Exp_2UA was bonded in E&R mode **(A)**. Exp-2UA's zinc-calcium-fluoride bioglass **(B)**. Potential anti-MMP **(C)** and anti-bacterial **(D)** effect attributed to gradual Zn release. The 'immediate' 1w and 'aged' 1y bond strength of Exp_2UA used in E&R bonding mode **(E)**. Schematic detailing the interfacial ultra-structure resulting when Exp_2UA was bonded in SE mode **(F).** The nano-layering structures observed at Exp_2UA's adhesive-dentin interface were stable upon 1y water storage **(G)**. The 'immediate' 1w and 'aged' 1y bond strength of Exp_2UA used in SE bonding mode **(H)**. Ar: adhesive resin; Hy: hybrid layer; Rt: resin tag; Ud: unaffected dentin.

■ ASSOCIATED CONTENT

Supporting Information

The Supporting Information is available free of charge on the ACS Publications website.

List of adhesives investigated in this study following the two bonding modes; measurement for water sorption and solubility; preparation of smear layer and μ-specimens for μTBS testing; overview (S)TEMs illustrating the filler-matrix configuration of BZF-21.

■ AUTHOR INFORMATION

Corresponding Author

*E-mail: bart.vanmeerbeek@kuleuven.be (Bart Van Meerbeek)

Notes

The authors declare no competing financial interest.

■ ACKNOWLEDGEMENTS

GC Europe is gratefully acknowledged for collaborating to produce the experimental adhesive and providing other commercial adhesives and composites. C. Yao's research stay and research conducted at BIOMAT of KU Leuven was partially supported by the China Scholarship Council (File No. 201706270148). JV is a postdoctoral fellow of the Research Foundation of Flanders (FWO Vlaanderen, mandate 12Z0920N) and is financially supported by KU Leuven through a C1 grant (C16/17/010) and FWO-Vlaanderen grant (G0A3820N). FZ is a postdoctoral fellow of the FWO Vlaanderen (mandate 12S8418N). The authors deny any conflicts of interest related to this study.

■ REFERENCES

(1) Van Meerbeek, B.; Vargas, M.; Inoue, S.; Yoshida, Y.; Peumans, M.; Lambrechts, P.; Vanherle, G. Adhesives and Cements to Promote Preservation Dentistry. *Oper. Dent.* **2001**, *Suppl 6,* 119-144.

(2) Pashley, D. H.; Tay, F. R.; Breschi, L.; Tjaderhane, L.; Carvalho, R. M.; Carrilho, M.; Tezvergil-Mutluay, A. State of the Art Etch-and-Rinse Adhesives. *Dent. Mater.* **2011,** *27*, 1-16.

(3) Van Meerbeek, B.; Yoshihara, K.; Yoshida, Y.; Mine, A.; De Munck, J.; Van Landuyt, K. L. State of the Art of Self-Etch Adhesives. *Dent. Mater.* **2011,** *27*, 17-28.

(4) Van Meerbeek, B.; Yoshihara, K.; Van Landuyt, K.L.; Yoshida, Y.; Peumans, M. From Buonocore's

Pioneering Acid-Etch Technique to Self-Adhering Restoratives. A Status Perspective of Rapidly Advancing Dental Adhesive Technology. *J. Adhes. Dent.* **2020,** *22*, 7-34.
(5) Nagarkar, S.; Theis-Mahon, N.; Perdigão, J. Universal Dental Adhesives: Current Status, Laboratory Testing, and Clinical Performance. *J. Biomed. Mater. Res. B. Appl. Biomater.* **2019,** *107*, 2121-2131.
(6) Van Landuyt, K.L.; Mine, A.; De Munck, J.; Jaecques, S.; Peumans, M.; Lambrechts, P; Van Meerbeek, B. Are One-Step Adhesives Easier to Use and Better Performing?Multifactorial Assessment of Contemporary One-Step Self-Etching Adhesives. *J. Adhes. Dent.* **2009,** *11*, 175-190.
(7) Peumans, M.; Kanumilli, P.; De Munck, J.; Van Landuyt, K.L.; Lambrechts, P.; Van Meerbeek, B. Clinical Effectiveness of Contemporary Adhesives: A Systematic Review of Current Clinical Trials. *Dent. Mater.* **2005,** *21*, 864-881.
(8) Breschi, L.; Mazzoni, A.; Ruggeri, A.; Cadenaro, M.; Di Lenarda, R.; De Stefano Dorigo, E. Dental Adhesion Review: Aging and Stability of the Bonded Interface. *Dent. Mater.* **2008,** *24*, 90-101.
(9) Perdigão, J.; Muñoz, M. A.; Sezinando, A.; Luque-Martinez, I. V.; Staichak, R.; Reis, A.; Loguercio, A. D. Immediate Adhesive Properties to Dentin and Enamel of a Universal Adhesive Associated With a Hydrophobic Resin Coat. *Oper. Dent.* **2014,** *39*, 489-499.
(10) Ahmed, M. H.; De Munck, J.; Van Landuyt, K.L.; Peumans, M.; Yoshihara, K.; Van Meerbeek, B. Do Universal Adhesives Benefit from an Extra Bonding Layer? *J. Adhes. Dent.* **2019,** *21*, 117-132.
(11) De Munck, J.; Van Landuyt, K.L.; Peumans, M.; Poitevin, A.; Lambrechts, P.; Braem, M.; Van Meerbeek, B. A Critical Review of the Durability of Adhesion to Tooth Tissue: Methods and Results. *J. Dent. Res.* **2005,** *84*, 118-132.
(12) Liu, Y.; Tjäderhane, L.; Breschi, L.; Mazzoni, A.; Li, N.; Mao, J.; Pashley, D. H.; Tay, F. R. Limitations in Bonding to Dentin and Experimental Strategies to Prevent Bond Degradation. *J. Dent. Res.* **2011,** *90*, 953-968.
(13) Mazzoni, A.; Tjäderhane, L.; Checchi, V.; Di Lenarda, R.; Salo, T.; Tay, F. R.; Pashley, D. H.; Breschi, L. Role of Dentin MMPs in Caries Progression and Bond Stability. *J. Dent. Res.* **2014,** *94*, 241-251.
(14) Mazzoni, A.; Scaffa, P.; Carrilho, M.; Tjäderhane, L.; Di Lenarda, R.; Polimeni, A.; Tezvergil-Mutluay, A.; Tay, F. R.; Pashley, D. H.; Breschi, L. Effects of Etch-and-Rinse and Self-etch Adhesives on Dentin MMP-2 and MMP-9. *J. Dent. Res.* **2012,** *92*, 82-86.
(15) De Munck, J.; Van den Steen, P. E.; Mine, A.; Van Landuyt, K. L.; Poitevin, A.; Opdenakker, G.; Van Meerbeek, B. Inhibition of Enzymatic Degradation of Adhesive-Dentin Interfaces. *J. Dent. Res.* **2009,** *88*, 1101-1106.
(16) Tjäderhane, L.; Nascimento, F. D.; Breschi, L.; Mazzoni, A.; Tersariol, I. L.; Geraldeli, S.; Tezvergil-Mutluay, A.; Carrilho, M. R.; Carvalho, R. M.; Tay, F. R.; Pashley, D. H. Optimizing Dentin Bond Durability: Control of Collagen Degradation by Matrix Metalloproteinases and Cysteine Cathepsins. *Dent. Mater.* **2013,** *29*, 116-135.
(17) Sulkala, M.; Tervahartiala, T.; Sorsa, T.; Larmas, M.; Salo, T.; Tjaderhane, L. Matrix Metalloproteinase-8 (MMP-8) is the Major Collagenase in Human Dentin. *Arch. Oral. Biol.* **2007,** *52*, 121-127.
(18) Perdigão, J.; Reis, A.; Loguercio, A. D. Dentin Adhesion and MMPs: A Comprehensive Review. *J. Esthet. Restor. Dent.* **2013,** *25*, 219-241.
(19) Seseogullari-Dirihan, R.; Apollonio, F.; Mazzoni, A.; Tjäderhane, L.; Pashley, D.; Breschi, L.; Tezvergil-Mutluay, A. Use of Crosslinkers to Inactivate Dentin MMPs. *Dent. Mater.* **2016,** *32*, 423-432.
(20) Tezvergil-Mutluay, A.; Agee, K. A.; Hoshika, T.; Carrilho, M.; Breschi, L.; Tjäderhane, L.; Nishitani, Y.; Carvalho, R. M.; Looney, S.; Tay, F. R.; Pashley, D. H. The Requirement of Zinc and Calcium Ions for

Functional MMP Activity in Demineralized Dentin Matrices. *Dent. Mater.* **2010,** *26*, 1059-1067.
(21) Altinci, P.; Seseogullari-Dirihan, R.; Can, G.; Pashley, D.; Tezvergil-Mutluay, A. Zinc Inhibits Collagenolysis by Cathepsin K and Matrix Metalloproteinases in Demineralized Dentin Matrix. *Caries. Res.* **2018,** *51*, 576-581.
(22) De Souza, A. P.; Gerlach, R. F.; Line, S. R. P. Inhibition of Human Gingival Gelatinases (MMP-2 and MMP-9) by Metal Salts. *Dent. Mater.* **2000,** *16*, 103-108.
(23) Osorio, R.; Yamauti, M.; Osorio, E.; Ruiz-Requena, M. E.; Pashley, D. H.; Tay, F. R.; Toledano, M. Zinc Reduces Collagen Degradation in Demineralized Human Dentin Explants. *J. Dent.* **2011,** *39*, 148-153.
(24) Nedeljkovic, I.; De Munck, J.; Vanloy, A.; Declerck, D.; Lambrechts, P.; Peumans, M.; Teughels, W.; Van Meerbeek, B.; Van Landuyt, K. L. Secondary Caries: Prevalence, Characteristics, and Approach. *Clin. Oral. Investig.* **2020,** *24*, 683-691.
(25) Tezvergil-Mutluay, A.; Agee, K. A.; Uchiyama, T.; Imazato, S.; Mutluay, M. M.; Cadenaro, M.; Breschi, L.; Nishitani, Y.; Tay, F. R.; Pashley, D. H. The Inhibitory Effects of Quaternary Ammonium Methacrylates on Soluble and Matrix-bound MMPs. *J. Dent. Res.* **2011,** *90*, 535-540.
(26) Chen, L.; Suh, B. I.; Yang, J. Antibacterial Dental Restorative Materials: A Review. *Am. J. Dent.* **2018,** *31*, 6B-12B.
(27) Almoudi, M. M.; Hussein, A. S.; Abu Hassan, M. I.; Mohamad Zain, N. A Systematic Review on Antibacterial Activity of Zinc Against Streptococcus Mutans. *Saudi. Dent. J.* **2018,** *30*, 283-291.
(28) Wiegand, A.; Buchalla, W.; Attin, T. Review on Fluoride-Releasing Restorative Materials--Fluoride Release and Uptake Characteristics, Antibacterial Activity and Influence on Caries Formation. *Dent. Mater.* **2007,** *23*, 343-362.
(29) Yao, C.; Ahmed, M. H.; Yoshihara, K.; Mercelis, B.; Parise Gré, C.; Van Landuyt, K. L.; Huang, C.; Van Meerbeek, B. Bonding to Enamel Using Alternative Enamel Conditioner/Etchants. *Dent. Mater.* **2019,** *35*, 1415-1429.
(30) Yoshihara, K.; Nagaoka, N.; Maruo, Y.; Sano, H.; Yoshida, Y.; Van Meerbeek, B. Bacterial Adhesion Not Inhibited by Ion-releasing Bioactive Glass Filler. *Dent. Mater.* **2017,** *33*, 723-734.
(31) Ito, S.; Hoshino, T.; Iijima, M.; Tsukamoto, N.; Pashley, D. H.; Saito, T. Water Sorption/Solubility of Self-Etching Dentin Bonding Agents. *Dent. Mater.* **2010,** *26*, 617-626.
(32) Zankuli, M. A.; Devlin, H.; Silikas, N. Water Sorption and Solubility of Core Build-Up Materials. *Dent. Mater.* **2014,** *30*, e324-329.
(33) International Standards Organization. ISO standard 4049:2019(E). Dentistry-polymer-based restorative materials. Geneva, Switzerland. **2019**. p.19-21.
(34) Pongprueksa, P.; Miletic, V.; Janssens, H.; Van Landuyt, K. L.; De Munck, J.; Godderis, L.; Van Meerbeek, B. Degree of Conversion and Monomer Elution of CQ/Amine and TPO Adhesives. *Dent. Mater.* **2014,** *30*, 695-701.
(35) Inokoshi, M.; Pongprueksa, P.; De Munck, J.; Zhang, F.; Vanmeensel, K.; Minakuchi, S.; Vleugels, J.; Naert, I.; Van Meerbeek, B. Influence of Light Irradiation Through Zirconia on the Degree of Conversion of Composite Cements. *J. Adhes. Dent.* **2016,** *18*, 161-171.
(36) Pongprueksa, P.; De Munck, J.; Inokoshi, M.; Van Meerbeek, B. Polymerization Efficiency Affects Interfacial Fracture Toughness of Adhesives. *Dent. Mater.* **2018,** *34*, 684-692.
(37) Armstrong, S.; Breschi, L.; Ozcan, M.; Pfefferkorn, F.; Ferrari, M.; Van Meerbeek, B. Academy of Dental Materials Guidance on in Vitro Testing of Dental Composite Bonding Effectiveness to Dentin/Enamel Using Micro-Tensile Bond Strength (μTBS) Approach. *Dent. Mater.* **2017,** *33*, 133-143.
(38) Van Meerbeek, B.; Yoshida, Y.; Lambrechts, P.; Vanherle, G.; Duke, E. S.; Eick, J. D.; Robinson, S. J. A

TEM Study of Two Water-Based Adhesive Systems Bonded to Dry and Wet Dentin. *J. Dent. Res.* **1998,** *77*, 50-59.
(39) Vandooren, J.; Geurts, N.; Martens, E.; Van den Steen, P.E.; De Jonghe, S.; Herdewijn, P.; Opdenakker, G. Gelatin Degradation Assay Reveals MMP-9 Inhibitors and Function of O-Glycosylated Domain. *World. J. Biol. Chem.* **2011,** *2*, 14-24.
(40) Nedeljkovic, I.; De Munck, J.; Ungureanu, A. A.; Slomka, V.; Bartic, C.; Vananroye, A.; Clasen, C.; Teughels, W.; Van Meerbeek, B.; Van Landuyt, K. L. Biofilm-Induced Changes to the Composite Surface. *J. Dent.* **2017,** *63*, 36-43.
(41) Davis, H. B.; Gwinner, F.; Mitchell, J. C.; Ferracane, J. L. Ion Release From, and Fluoride Recharge of a Composite with a Fluoride-Containing Bioactive Glass. *Dent. Mater.* **2014,** *30*, 1187-1194.
(42) Ito, S.; Hashimoto, M.; Wadgaonkar, B.; Svizero, N.; Carvalho, R. M.; Yiu, C.; Rueggeberg, F. A.; Foulger, S.; Saito, T.; Nishitani, Y.; Yoshiyama, M.; Tay, F. R.; Pashley, D. H. Effects of Resin Hydrophilicity on Water Sorption and Changes in Modulus of Elasticity. *Biomaterials.* **2005,** *26*, 6449-6459.
(43) Reis, A. F.; Giannini, M.; Pereira, P. N. Influence of Water-Storage Time on the Sorption and Solubility Behavior of Current Adhesives and Primer/Adhesive Mixtures. *Oper Dent* **2007,** *32*, 53-59.
(44) Prime&Bond Active Universal Adhesive Scientific Compendium, Dentsply Sirona, Konstanz, Germany.
(45) Salz, U.; Zimmermann, J.; Zeuner, F.; Moszner, N. Hydrolytic Stability of Self-etching Adhesive Systems. *J. Adhes. Dent.* **2005,** *7*, 107-116.
(46) Hashimoto, M.; Ohno, H.; Kaga, M.; Endo, K.; Sano, H.; Oguchi, H. In Vivo Degradation of Resin-Dentin Bonds in Humans Over 1 to 3 Years. *J. Dent. Res.* **2000,** *79*, 1385-1391.
(47) Wei, Y. J.; Silikas, N.; Zhang, Z. T.; Watts, D. C. Diffusion and Concurrent Solubility of Self-Adhering and New Resin-Matrix Composites During Water Sorption/Desorption Cycles. *Dent. Mater.* **2011,** *27*, 197-205.
(48) Hass, V.; Dobrovolski, M.; Zander-Grande, C.; Martins, G. C.; Gordillo, L. A.; Rodrigues Accorinte Mde, L.; Gomes, O. M.; Loguercio, A. D.; Reis, A. Correlation Between Degree of Conversion, Resin-Dentin Bond Strength and Nanoleakage of Simplified Etch-and-Rinse Adhesives. *Dent. Mater.* **2013,** *29*, 921-928.
(49) Clearfil SE Bond 2 technical information, Kuraray Noritake, Tokyo, Japan.
(50) Sato, K.; Hosaka, K.; Takahashi, M.; Ikeda, M.; Tian, F.; Komada, W.; Nakajima, M.; Foxton, R.; Nishitani, Y.; Pashley, D. H.; Tagami, J. Dentin Bonding Durability of Two-step Self-etch Adhesives with Improved of Degree of Conversion of Adhesive Resins. *J. Adhes. Dent.* **2017,** *19*, 31-37.
(51) De Munck, J.; Mine, A.; Poitevin, A.; Van Ende, A.; Cardoso, M. V.; Van Landuyt, K. L.; Peumans, M.; Van Meerbeek, B. Meta-Analytical Review of Parameters Involved in Dentin Bonding. *J. Dent. Res.* **2012,** *91*, 351-357.
(52) Ahmed, M.H.; Yoshihara, K.; Mercelis, B.; Van Landuyt, K.L.; Peumans, M.; Van Meerbeek, B. Quick Bonding Using a Universal Adhesive. *Clin. Oral. Investig.* **2019**, [Epub ahead of print].
(53) Ausiello, P.; Apicella, A.; Davidson, C. L. Effect of Adhesive Layer Properties on Stress Distribution in Composite Restorations--A 3D Finite Element Analysis. *Dent. Mater.* **2002,** *18*, 295-303.
(54) Van Meerbeek, B.; Willems, G.; Celis, J. P.; Roos, J. R.; Braem, M.; Lambrechts, P.; Vanherle, G. Assessment by Nano-Indentation of the Hardness and Elasticity of the Resin-Dentin Bonding Area. *J. Dent. Res.* **1993,** *72*, 1434-1442.
(55) Van Landuyt, K. L.; De Munck, J.; Mine, A.; Cardoso, M. V.; Peumans, M.; Van Meerbeek, B. Filler Debonding & Subhybrid-Layer Failures in Self-Etch Adhesives. *J. Dent. Res.* **2010,** *89*, 1045-1050.

(56) Yoshihara, K.; Nagaoka, N.; Yoshida, Y.; Van Meerbeek, B.; Hayakawa, S. Atomic Level Observation and Structural Analysis of Phosphoric-Acid Ester Interaction at Dentin. *Acta. Biomater.* **2019,** *97*, 544-556.
(57) Yoshihara, K.; Yoshida, Y.; Nagaoka, N.; Fukegawa, D.; Hayakawa, S.; Mine, A.; Nakamura, M.; Minagi, S.; Osaka, A.; Suzuki, K.; Van Meerbeek, B. Nano-Controlled Molecular Interaction at Adhesive Interfaces for Hard Tissue Reconstruction. *Acta. Biomater.* **2010,** *6*, 3573-3582.
(58) Birkedal-Hansen, H. Proteolytic Remodeling of Extracellular Matrix. *Current. Opinion. Cell. Bio.* **1995,** *7*, 728-735.
(59) Tay, F. R.; Pashley, D. H.; Loushine, R. J.; Weller, R. N.; Monticelli, F.; Osorio, R. Self-Etching Adhesives Increase Collagenolytic Activity in Radicular Dentin. *J. Endod.* **2006,** *32*, 862-868.
(60) Chaussain-Miller, C.; Fioretti, F.; Goldberg, M.; Menashi, S. The Role of Matrix Metalloproteinases (Mmps) in Human Caries. *J. Dent. Res.* **2006,** *85*, 22-32.
(61) Sauro, S.; Osorio, R.; Fulgêncio, R.; Watson, T. F.; Cama, G.; Thompson, I.; Toledano, M. Remineralisation Properties of Innovative Light-curable Resin-based Dental Materials Containing Bioactive Micro-fillers. *J. Mater. Chem. B.* **2013,** *1*, 2624-2638.
(62) Osorio, R.; Yamauti, M.; Sauro, S.; Watson, T. F.; Toledano, M. Zinc Incorporation Improves Biological Activity of Beta-tricalcium Silicate Resin–based Cement. *J. Endod.* **2014,** *40*, 1840-1845.
(63) Van Meerbeek, B. Mechanisms of Resin Adhesion: Dentin&Enamel Bonding, *J. Esthet. Restor. Dent.* **2008**, *2*, 2-8.
(64) Nedeljkovic, I.; De Munck, J.; Slomka, V.; Van Meerbeek, B.; Teughels, W.; Van Landuyt, K. L. Lack of Buffering by Composites Promotes Shift to More Cariogenic Bacteria. *J. Dent. Res.* **2016,** *95*, 875-881.
(65) Matsuo, K.; Yoshihara, K.; Nagaoka, N.; Makita, Y.; Obika, H.; Okihara, T.; Matsukawa, A.; Yoshida, Y.; Van Meerbeek, B. Rechargeable Anti-Microbial Adhesive Formulation Containing Cetylpyridinium Chloride Montmorillonite. *Acta. Biomater.* **2019,** *100*, 388-397.
(66) Metwalli, K. H.; Khan, S. A.; Krom, B. P.; Jabra-Rizk, M. A. Streptococcus Mutans, Candida Albicans, and The Human Mouth: A Sticky Situation. *PLoS. Pathog.* **2013,** *9*, e1003616.1- e1003616.5.
(67) Lynch, R. J. Zinc in the Mouth, Its Interactions with Dental Enamel and Possible Effects on Caries; A Review of the Literature. *Int. Dent. J.* **2011,** *61 Suppl 3*, 46-54.
(68) Liu, Y.; Kohno, T.; Tsuboi, R.; Kitagawa, H.; Imazato, S. Acidity-Induced Release of Zinc Ion From Biounion$^{(TM)}$ Filler and Its Inhibitory Effects Against Streptococcus Mutans. *Dent. Mater. J.* **2020**, [Epub ahead of print].
(69) Hamilton IR, E. D. Effects of Fluoride on Carbohydrate Metabolism by Washed Cells of Streptococcus Mutans Grown at Various pH Values in a Chemostat. *Infect. Immun.* **1978,** *19*, 434-442.

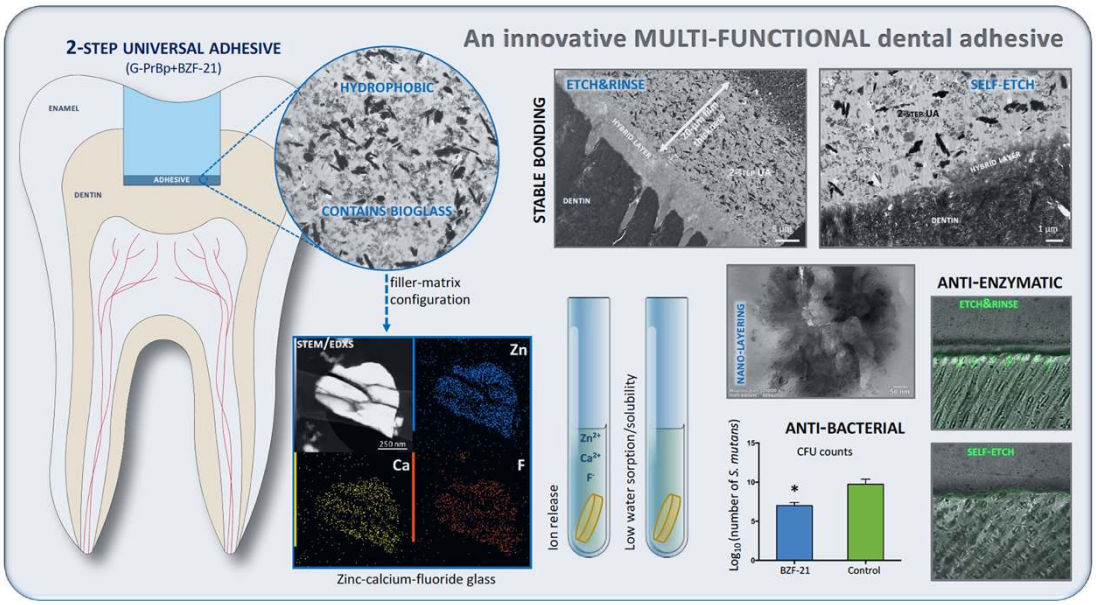

For Table of Contents only.

Supporting Information

Zinc-calcium-fluoride bioglass-based innovative multi-functional dental adhesive with thick adhesive-resin film thickness

Chenmin Yao,[†,‡] Mohammed H. Ahmed,[†,§] Xin Li,[†] Ivana Nedeljkovic,[†,//] Jennifer Vandooren,[#] Ben Mercelis,[†] Fei Zhang,[†,&] Kirsten L. Van Landuyt,[†] Cui Huang,[‡] Bart Van Meerbeek[†,*]

[†]KU Leuven (University of Leuven), Department of Oral Health Sciences, BIOMAT & UZ Leuven (University Hospitals Leuven), Dentistry, 3000 Leuven, Belgium;

[‡]Wuhan University, the State Key Laboratory Breeding Base of Basic Science of Stomatology (Hubei-MOST) & Key Laboratory of Oral Biomedicine Ministry of Education (KLOBM), School & Hospital of Stomatology, 430079 Wuhan, China;

[§]Tanta University, Faculty of Dentistry, Department of Dental Biomaterials, 31511 Tanta, Egypt;

[//]University of Amsterdam and Vrije Universiteit Amsterdam, Department of Dental Material Sciences, Academic Centre for Dentistry Amsterdam (ACTA), 1081 LA Amsterdam, The Netherlands;

[#]KU Leuven (University of Leuven), Laboratory of Immunobiology, Rega Institute for Medical Research, 3000 Leuven, Belgium;

[&]KU Leuven (University of Leuven), Department of Materials Engineering, 3001 Leuven, Belgium.

*Corresponding author: bart.vanmeerbeek@kuleuven.be (Bart Van Meerbeek).

CONTENT

1. TABLE S1. .....S-3

2. EXPERIMENTAL SECTION S-5

2.1. Water sorption and solubility S-5

2.2. Preparation of smear layer S-5

2.3. Preparation of (μ)-specimens S-5

2.4. Actual μTBS testing S-6

3. RESULT S-7

REFERENCES S-8

Table S1. List of adhesives investigated in this study following the two bonding modes.

Adhesive	Code	Composition	Etch-and-rinse (E&R)	Self-etch (SE)
BZF-21 (GC, Tokyo, Japan)	**BZF-21**	BisGMA, UDMA, glycerol 1,3-dimethacrylate, camphorquinone, diphenyl (2,4,6-trimethylbenzoyl) phosphine oxide, polymerization inhibitor, zinc-calcium-fluoride glass, fumed silica	**1.** Etch dentin with K-Etchant Syringe (Kuraray Noritake) for 15 s, rinse for 5 s and gently air-dry; **2.** Apply G-PrBp using a microbrush, leave undisturbed for 10 s after the end of application; **3.** Dry thoroughly for 5 s with oil free air under maximum air pressure; **4.** Apply BZF-21, air-blow to make a thin layer with gentle air pressure; **5.** Light-cure using a high-power LED for 10 s.	**1.** Apply G-PrBp using a microbrush, leave undisturbed for 10 s after the end of application; **2.** Dry thoroughly for 5 s under maximum air pressure; **3.** Apply BZF-21, air-blow to make a thin layer with gentle air pressure; **4.** Light-cure using a high-power LED for 10 s.
G-Premio Bond (GC, Tokyo, Japan)	**G-PrB**	10-MDP, 4-MET, MDTP, methacrylate acid ester, distilled water, acetone, photo-initiators, silica fine powder	**1.** Etch dentin with K-Etchant Syringe for 15 s, rinse for 5 s and gently air-dry; **2.** Apply G-PrB using a microbrush, leave undisturbed for 10 s after the end of application; **3.** Dry thoroughly for 5 s with oil free air under maximum air pressure; **4.** Light-cure using a high-power LED for 10 s.	**1.** Apply G-PrB using a microbrush, leave undisturbed for 10 s after the end of application; **2.** Dry thoroughly for 5 s with oil-free air under maximum air pressure; **3.** Light-cure using a high-power LED for 10 s.
Prime&Bond Active (Dentsply Sirona, Konstanz, Germany)	**P&Ba**	10-MDP, PENTA, bi- and multifunctional acrylate, initiator, stabilizer, water, isopropanol	**1.** Etch dentin with K-Etchant Syringe for 15 s, rinse for 5 s and gently air-dry; **2.** Apply P&Ba to dentin and keep it slightly agitated for 20 s; **3.** Evaporate solvent with air for at least 5 s; **4.** Light-cure using a high-power LED for 10 s.	**1.** Apply P&Ba to dentin and keep it slightly agitated for 20 s; **2.** Evaporate solvent with air for at least 5 s; **3.** Light-cure using a high-power LED for 10 s.

Scotchbond Universal (3M Oral Care, Seefeld, Germany)	**SBU**	10-MDP, HEMA, silane, dimethacrylate resins, Vitrebond co-polymer, filler, ethanol, water, initiators	**1.** Etch dentin with K-Etchant Syringe for 15 s, rinse for 5 s and gently air-dry; **2.** Apply SBU to dentin and rub it in for 20 s; **3.** Gently air-dry for 5 s; **4.** Light-cure using a high-power LED for 10 s.	**1.** Apply SBU to dentin and rub it in for 20 s; **2.** Gently air-dry for 5 s; **3.** Light-cure using a high-power LED for 10 s.
Clearfil SE Bond 2 (Kuraray Noritake, Tokyo, Japan)	**CSE2**	Primer: 10-MDP, HEMA, hydrophilic aliphatic dimethacrylate, dl-camphorquinone, accelerators Adhesive resin: BisGMA, 10-MDP, HEMA, hydrophobic aliphatic dimethacrylate, dl-camphorquinone, initiators, silanated colloidal silica, accelerators	**1.** Etch dentin with K-Etchant Syringe for 15 s, rinse for 5 s and gently air-dry; **2**. Apply CSE2 Primer using a microbrush, leaving it in place for 20 s prior to being mildly air-dried for more than 5 s; **3.** Apply CSE2 Bond, followed by gentle air-drying; **4.** Light-cure using a high-power LED for 10 s.	**1.** Apply CSE2 Primer using a microbrush, followed by leaving it in place for 20 s prior to being mildly air-dried for more than 5 s; **2.** Apply CSE2 Bond, followed by gentle air-drying; **3.** Light-cure using a high-power LED for 10 s.

4-MET: 4-methacryloyloxyethyl trimellitate anhydrate; 10-MDP: methacryloxydecyl dihydrogen phosphate; BisGMA: bisphenol A diglycidylmethacrylate; HEMA: 2-hydroxyethyl methacrylate; MDTP: methacryoyloxydecyl dihydrogen thiophosphate; PENTA: dipentaerythritol pentacrylate phosphate; UDMA: urethane dimethacrylate.

2. Experimental section

2.1. Water sorption and solubility

The top and bottom surfaces were wet ground with P1200 SiC paper to adjust the disk thickness. Disk dimensions to the nearest 0.01 mm were measured using a digital caliper (Mitutoyo Absolute 500-181-20, Mitutoyo Corporation, Sakado, Kanagawa, Japan). The volume (V) of each disc was calculated in mm^3. The specimens were placed in a 37°C incubator for 22h, then allowed to cool off to 23°C (room temperature) for 2h and weighed to an accuracy of 0.01 mg using a calibrated electronic analytical balance. The specimens were maintained in a desiccator and re-weighed every 24h until a constant mass, referred to as 'm1' was reached. Specimens of each adhesive were next immersed in 10 ml distilled water in individual glass containers for 1w. One third of the specimens (n=3) of each adhesive were gently dried, waved in air for 15s and re-weighed to an accuracy of 0.01 mg, being referred to as 'm2'. Then, these specimens were dried to a constant mass, referred to as 'm3', in a desiccator for 1w. The additional remaining six specimens of each adhesive were left in distilled water for 6m and 1y, and again dried until the constant mass 'm3' was reached.

2.2. Preparation of smear layer

A standard smear layer was produced using a medium-grit (107 µm) diamond bur (882, Komet, Lemgo, Germany) mounted in the MicroSpecimen Former (University of Iowa, Iowa, IA, USA).[1] All dentin surfaces were carefully verified for absence of enamel and/or pulp tissue using a stereomicroscope (Stemi 2000-CS, Zeiss, Oberkochen, Germany).

2.3. Preparation of (µ)-specimens

The primer/adhesive resin was applied onto the bur-cut dentin surface strictly following the respective manufacturer's instructions (Table S1). After adhesive procedures, the surfaces were built up with the micro-hybrid composite Z100 (3M Oral Care) in three layers up to a height of 5 mm. Each increment of

max. 2 mm was light cured for 20s using the LED-curing light Bluephase 20i (Ivoclar Vivadent) with an output of 1200 mW/cm^2. Upon completion, the composite block was additionally light cured for 20s from each side, so to ensure optimum curing. Thereafter, the bonded specimens were immediately stored for 1w in distilled water at 37°C.

Upon 1-w water storage, all specimens were sectioned perpendicular to the interface using a water-cooled diamond saw (Accutom-50, Struers) to obtain rectangular sticks (12 micro (μ)-specimens per tooth: 1×1 mm wide; 8-9 mm long).

2.4. Actual μTBS testing

For the actual μTBS test, the specimens were fixed to a BIOMAT jig using cyanoacrylate-based glue (Model Repair II Blue, Dentsply Sankin, Tochigiken, Japan), upon which they were stressed at a crosshead speed of 1 mm/min until failure in a LRX testing device (LRX, Lloyd, Hampshire, UK) using a load cell of 100N.[1]

The mode of failure was determined under 50x magnification using a stereomicroscope (Stemi 2000-CS, Zeiss) and classified as either 'cohesive failure in dentin', 'cohesive failure in resin', 'adhesive (interfacial) failure', or 'mixed failure'.[2]

3. Result

Overview (S)TEMs illustrate the filler-matrix configuration of BZF-21

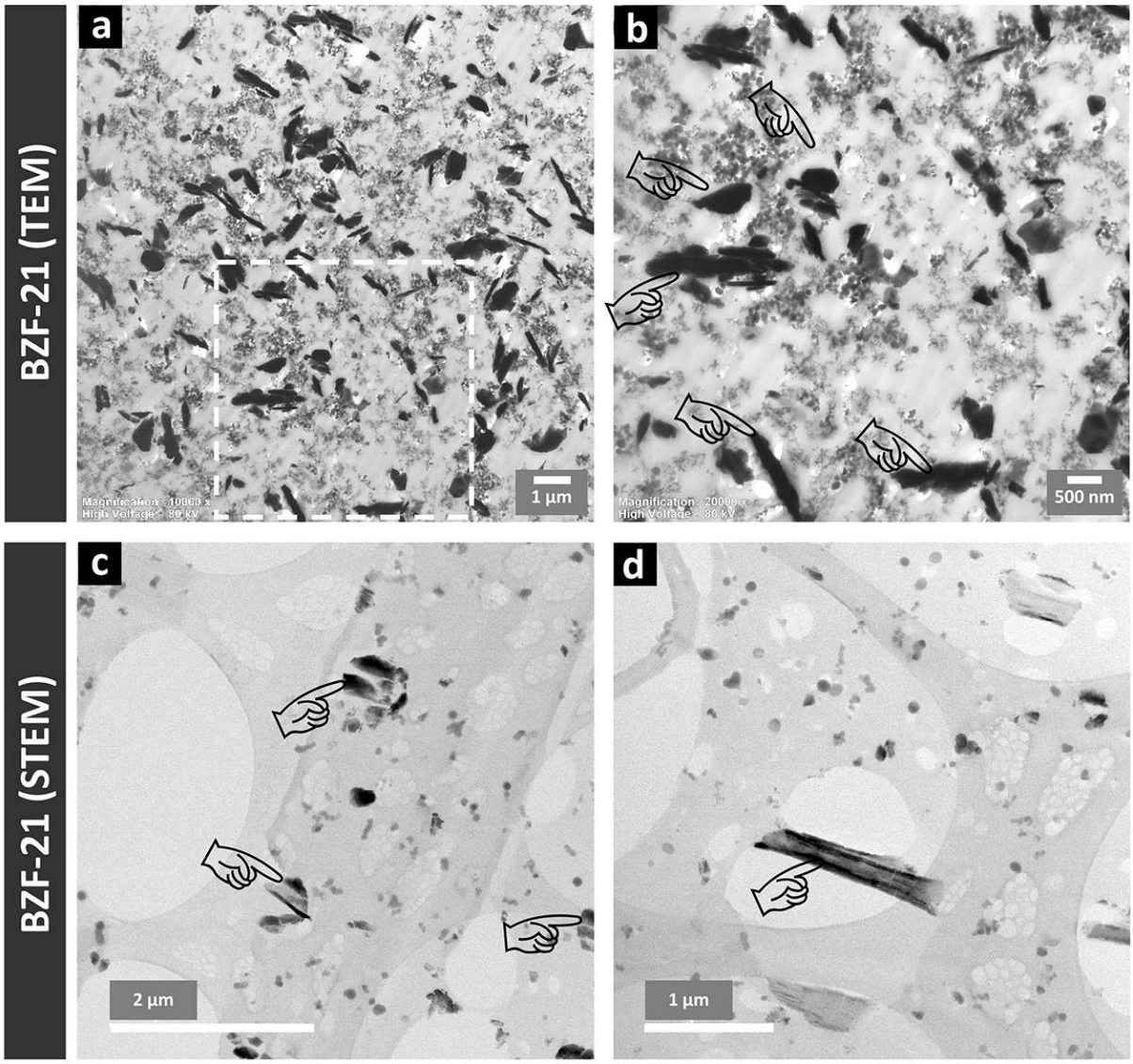

Figure S1. Overview TEMs (section thickness: 70-90 nm) of the filler-matrix configuration of the experimental multi-functional adhesive resin BZF-21 in **(a)**, with the white square magnified in **(b)**, both revealing zinc-calcium-fluoride bioglass filler particles with irregular shapes and homogenous distribution within the adhesive resin. Ultra-structural STEM photomicrographs (section thickness: 10-20 nm) of BZF-21's filler-matrix configuration in **(c,d)**, revealing Zn-Ca-F bioglass with mainly a size of around 250 nm. Handpointers: Zn-Ca-F bioglass filler particles.

References

(1) Yao, C.; Ahmed, M. H.; Yoshihara, K.; Mercelis, B.; Parise Gré, C.; Van Landuyt, K. L.; Huang, C.; Van Meerbeek, B. Bonding to Enamel Using Alternative Enamel Conditioner/Etchants. Dent. Mater. 2019, 35, 1415-1429.

(2) Yao, C.; Ahmed, M. H.; Zhang, F.; Mercelis, B.; Van Landuyt, K. L.; Huang, C.; Van Meerbeek, B. Structural/Chemical Characterization and Bond Strength of a New Self-Adhesive Bulk-fill Restorative. *J. Adhes. Dent.* **2020,** *22*, 85-97.